University of Cincinnati

Date: 4/2/2012

I, Siddharth Vaidyanathan , hereby submit this original work as part of the requirements for the degree of Master of Science in Materials Science.

It is entitled:

Electrochemical Characteristics of Conductive Polymer Composite based Supercapacitors

Student's name: **Siddharth Vaidyanathan**

This work and its defense approved by:

Committee chair: Relva Buchanan, ScD

Committee member: Rodney Roseman, PhD

Committee member: Dale Schaefer, PhD

2469

Electrochemical Characteristics of Conductive Polymer Composite based Supercapacitors

A thesis submitted to the division of Research and Advanced Studies at the University of Cincinnati in partial fulfillment of the requirement for the degree of

MASTER OF SCIENCE

In the School of Energy and Materials Engineering, College of Engineering and Applied Science

April, 2012

By, **Siddharth Vaidyanathan**

Committee Chair: Dr. Relva C Buchanan

School of Energy and Materials Engineering

University of Cincinnati, Cincinnati OH -45221

USA

Abstract

Supercapacitors are devices that store large amount of charge. Supercapacitors can play a key role in the drive towards a cleaner and greener environment. This research focuses on the properties of electrochemical cells and the application of conductive polymer composites as effective electrode materials in a supercapacitor. The effect of electrochemical cell parameters like distance of separation, electrolyte and separator material on the overall capacitance was studied. An innovative two electrode cell design was developed to facilitate these measurements. Conductive polymer composites were prepared using physical milling and pressed into pellets using hot pressing and normal pressing techniques. The characterization of conductive polymer composite electrode based supercapacitors was carried out using electrochemical impedance spectroscopy, cyclic voltammetry and chronopotentiometry. The performance of two polymers (polyaniline and acrylonitrile butadiene styrene) with different levels of conductivity was compared, in order to understand the double layer capacitance and pseudo-capacitance mechanisms. The surface properties, crystal structure and chemical composition were analyzed using scanning electron microscopy, energy dispersive spectroscopy and x-ray diffraction.

Acknowledgement

I would like thank my advisor Dr. Relva C Buchanan for the continuous guidance that he provided me through my Master's research work. I would also like to thank Dr. Dale W Schaefer and Dr Rodney Roseman for taking time to review my thesis and being a part of my defense committee.

It was a great pleasure working with my research group members: Arun Surendernath, Prabhu Megharaj, Xiang Gao, Harshani Tennakone, Yongkun Zhou, Yuxuan Gong and Dr. Kirthi Tennakone. Their support and help has been invaluable in the success of this work.

I would also like to thank my friends Charan Rajan, Karthik Kumaresan, Ananta Vidyarthi, Gokulakrishanan Ramamkrishnan, Kedharnath Sairam and others both in the USA and India for the encouragement they provided me.

I also want to express my sincere gratitude to my parents, brother and other family members who have been a constant source of support throughout my life.

Table of contents

List of figures and tables

Figures

INTRODUCTION

EXPERIMENTAL

RESULTS AND DISCUSSION

List of abbreviations

1. ABS – Acrylonitrile butadiene styrene
2. PANI – Polyaniline
3. EIS – Electrochemical impedance spectroscopy
4. CV – Cyclic voltammetry
5. H_2SO_4 – Sulfuric acid
6. KOH – Potassium hydroxide
7. SEM – Scanning electron microscope
8. XRD – X-ray diffraction

INTRODUCTION

1.1 Background

1.1.1 Energy and its usage

Energy is a basic need all societies. Energy can be of different types, namely kinetic energy, potential energy, solar energy and electrical energy. Automobiles, factories, electricity generation and other day to day activities are all dependent on a constant supply of energy. This energy originates from various sources like fossil fuels, sun, wind and water. The annual consumption of energy worldwide has been steadily increasing forcing societies everywhere to continuously look for newer sources of energy. Figure 1 below illustrates this trend and the widening gap of consumption over production in the United States.

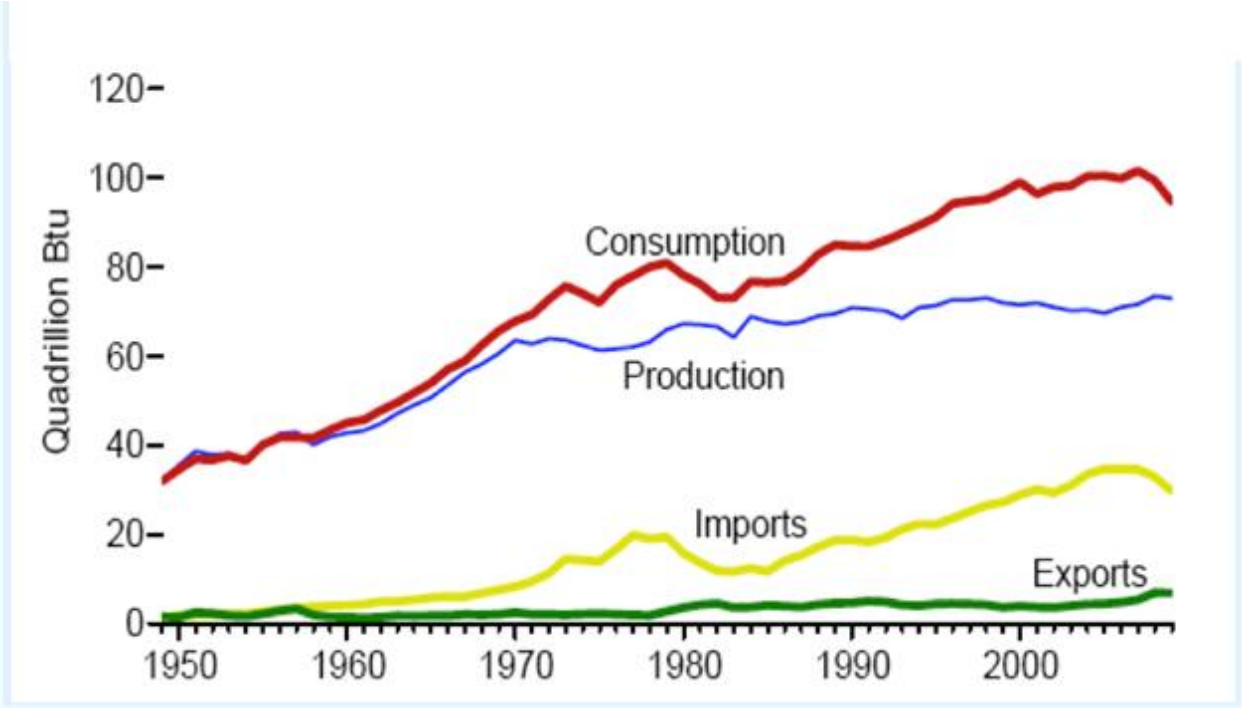

Figure 1: Energy consumption and production in the US [1]

In particular, figure 1 shows the increase in energy consumption in the US over the years. The continuous rise in energy consumption has a direct impact on the rapid increase in energy imports. While the United States was able to match its exports and imports until about 1965, the gap between consumption and production has been widening ever since. This has forced the United States to start importing energy, as current demand was not met with the available domestic energy sources.

1.1.2 Dependence on fossil fuels

Over the years, man has depended primarily on fossil fuels to satisfy his energy requirements. Fossil fuels are of three types mainly: coal, natural gas and oil. Fossil Fuels are considered non – renewable because they take a very long time to replenish. It is estimated that at the current rates of consuming fossil fuels, the available supply could be exhausted in a hundred years. With advancement in technology, the rate of energy consumption has risen rapidly to a point where we must develop alternate sources of energy to preserve existing resources.

There are many models that predict the depletion of fossil fuels, based on our current consumption trend. A modified Klass model predicts that, we will run out of coal, oil and natural gas in 107, 35 and 37 years respectively [2].

1.1.3 Alternate Sources of Energy

For sustained supply of energy over a long period of time, this picture has to change and we must move toward other energy sources that are renewable and have lesser impact on the environment. Efforts are being made to harness energy from renewable sources like sun, wind and water. These resources are available in plenty and there is no fear of running out of them.

Renewable sources however face some major issues that hamper their use on a large scale. Though these are environmentally friendly and do not have safety issues, lack of continuous availability is a major drawback [3]. Solar energy devices cannot be used in the night. Other disadvantages include low efficiency of these devices and high maintenance cost. Nuclear energy has some disadvantages. The cost of raw material is very high. Uranium and thorium are used in fission reactions and there is a lot of toxic waste that is generated. Disposal of the toxic waste is a major problem.

In recent times there is much interest in developing devices that store large amount of energy chemically and have high recyclability. Such devices include fuel cells, lithium-ion batteries and supercapacitors. They have a very low rate of degradation and are also environmentally friendly. The ability to develop these devices commercially to replace the existing lead based batteries will help in reducing pollution.

1.2 Supercapacitors

1.2.1 Background

Supercapacitor or ultra-capacitor is a device that has the ability to store large amount of energy when compared to a regular capacitor. Leyden jar was the first double layer capacitor to be developed. It was developed in 1746 in Leyden, Netherlands. But the first patent in this field was only in 1957 [4-6]. While conventional capacitors store charge ranging from a few microfarads to a few farads, supercapacitors can have capacities as high as 2000F/g. They pose a challenge to conventional batteries due to the power they can deliver, but low energy density storage has hindered their use in on a larger scale. Conventional capacitors use the dielectric mechanism to store charge, utilizing insulating materials with a high dielectric constant (e.g. barium titanate,)

which are sandwiched between two current collectors, resulting in charge storage on the face of the collectors. On the other hand, supercapacitors store charge based on charge separation mechanism or faradaic processes or both. High surface area electrode materials, with an electrolyte and separator in-between, comprise a standard supercapacitor cell structure.

Supercapacitors can be classified into two types: double layer capacitors and pseudo-capacitors. Charge storage in double layer capacitors is completely non-faradaic and involves movement of ions present in the electrolyte under the influence of an applied voltage. The positive ions move towards the negative electrode and the negative ions move towards the positive electrode, thus forming a double layer. In pseudo-capacitors energy is stored as a result of faradaic reactions between the electrode and the electrolyte. In double layer capacitors, the surface area of the electrodes plays an important role. On the other hand pseudo-capacitance is dependent mainly on voltage and dielectric constant values.

Figure 2 below is popularly called the Ragone Plot, it illustrates the relationship between energy and power densities for different energy storage devices that are commonly used. Fuel cells and conventional batteries have very high energy density but low power density. This limits their use, since they must be connected for high power applications. Electrolytic capacitors and supercapacitors exhibit very high power density but low energy density. While they are not able to store as much energy as batteries, they produce the stored energy in a short interval of time resulting in the supercapacitors having high power density. Much research effort is being directed, therefore, toward improving energy density of supercapacitors, as a realistic alternate to batteries.

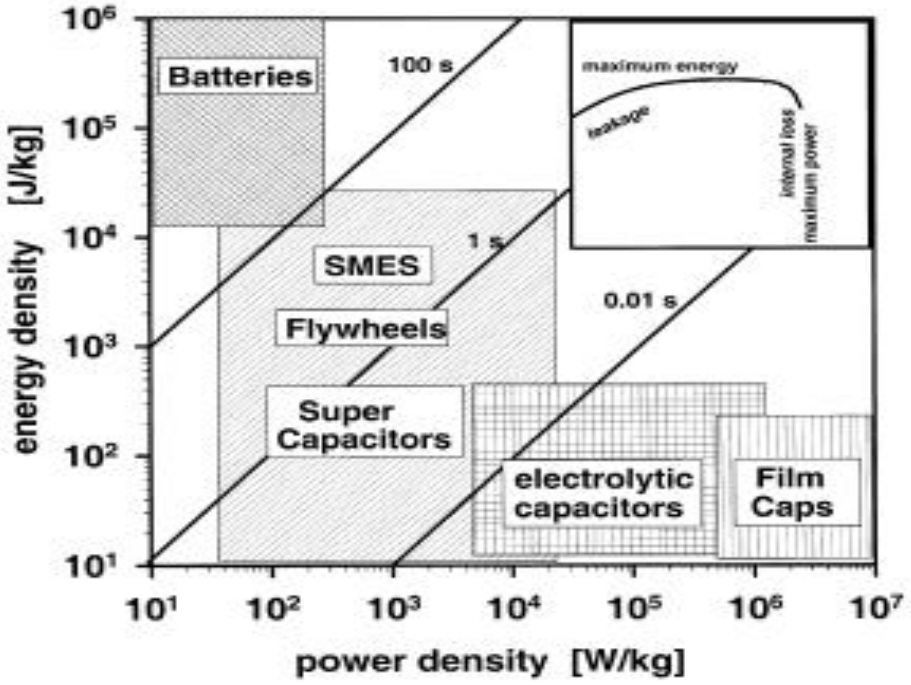

Figure 2: Ragone Plot [7]

1.2.2 Advantages and Disadvantages

Supercapacitors have many advantages over the existing energy devices like capacitors and batteries. As discussed, supercapacitors can be used in high power applications due to very high power density, good reversibility and, unlike batteries; they do not degrade much even when subjected to thousands of charge-discharge cycles. They are very easy to charge and can be charged rapidly. Supercapacitors are also considered to be environmental friendly due to their recyclability.

Supercapacitors, however, have disadvantages, which have hindered their development and widespread use. The low energy density limits their applications and use in situations where constant energy is required. For such applications, they are often coupled with batteries to help

improve the performance. The maximum voltage is very low and has to be connected in series to reach higher voltages [8].

1.2.3 Application

Supercapacitors are commonly used in series with batteries as a backup device. They can be used in hybrid vehicles, where the high power can be utilized to start engines, while the batteries provide the continuous energy required while the engine is running. They are also commonly used in high power devices, such as alarm clocks, computers, toys, and flashlights.

1.2.4 Factors affecting charge storage

The total capacitance of a supercapacitor depends on different factors that affect the charge storage. In this section, the roles of electrode material, electrolyte and separator on the overall performance of the cell, is examined.

Electrode Material

For double layer capacitors, the dominant energy storage mechanism is charge separation. The surface area of the electrode also plays a vital role. Materials having large surface area provide more active sites for ions in the electrolyte to form a double layer, resulting in more charge storage. The presence of porosity in the electrode material also aids electrolyte penetration into the electrode by enlarging the active surface area.. High surface area carbon, carbon nanotubes, and graphene are some of the materials that make good electrodes in double layer capacitors. Pseudo-capacitors store charge by a series of redox reactions. The doping and undoping process must occur rapidly for the energy to be delivered in short intervals. Polymers like polyaniline are commonly used as electrode materials in pseudo capacitors. The use of pure carbon materials can

affect the mechanical properties of the electrodes. Hence the electrodes are commonly blended with polymers to improve mechanical properties. Such capacitors rely on a combination of double layer capacitance and pseudo-capacitance [9].

Electrolyte

The electrolyte plays a key role in the energy storage mechanism of supercapacitors. The ions from the electrolyte migrate toward electrodes with opposite charge to form the double layer. The electrolyte must be chosen such that it does not affect the electrode surface over large number of cycles of charging and discharging. Organic electrolytes have a disassociation voltage of 2.5 V, compared to aqueous electrolytes, which disassociate at about 1.2V [10]. Some devices also use solid electrolytes which have even higher disassociation voltages. Tetraethyl ammonium terafluoro borate is a commonly used organic electrolyte. KOH and NaCl in water are some aqueous electrolytes that are used.

Battery Separator

The primary role of battery separators is to prevent contact between the two electrodes to prevent short circuit. The separator should be a good insulator but must also have very good permeability, to allow the ions in the electrolyte to pass through. The separator should exhibit good mechanical and chemical stability and have uniform thickness [11].

Distance of Separation

In the case of conventional capacitors, the distance of separation plays a crucial role in the overall capacitance as seen in equation below.

$$C = \frac{\epsilon_r \times k \times A}{d} \qquad (1)$$

Where

ϵ_r is the relative permittivity of the medium

k is the dielectric constant of the medium

A is the area of the electrode

d is the distance of electrode separation

From equation (1) we see that reducing the distance by half doubles the capacitance. The distance of separation is important in double layer capacitors as well. Although the capacitance does not directly depend on the distance of separation, as in the case conventional capacitors, with increasing separation between the electrodes the resistance will also increase, thus causing a decrease in capacitance. The electrodes must be as close to each as possible without touching.

1.3 Electrochemical Double Layer Theory

In 1879, Helmholtz first recognized the existence of a layer of charge or *double layer* formed on the surface of electrodes in an electrochemical system [12]. Following this, various theories have been proposed regarding the properties of the double layer. Figure 4 illustrates how charge is stored in a conventional capacitor and in an electrochemical double layer capacitor. In a double layer capacitor, under the influence of an external potential, the charges present in the electrolyte will become attracted to the electrodes with opposite charge and become adsorbed onto the

surface of the material. This creates a second layer of charge which is called the double layer, as illustrated in Figure 3 below.

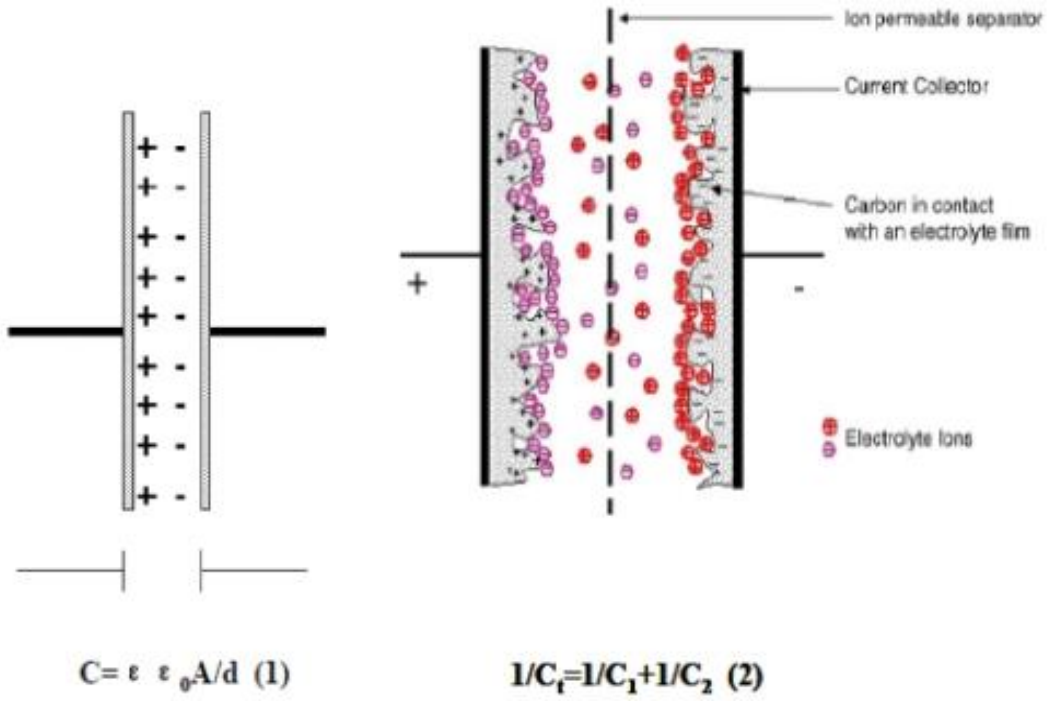

Figure 3: Conventional capacitor and electrochemical double layer capacitor [13]

1.3.1 Initial Ideas

Helmholtz proposed a simple theory, which states that ions in the electrolyte adsorb onto the surface of the current collectors in order to counter the charge at the surface. But this is an idealized concept and does not actually occur in this manner. Guoy and Chapman later suggested the presence of a diffuse layer where the counter ions are not rigidly held to surface but are gradiently diffused thoughout the solution, as illustrated in figure 4, below.

1.3.2 Stern Layer [12]

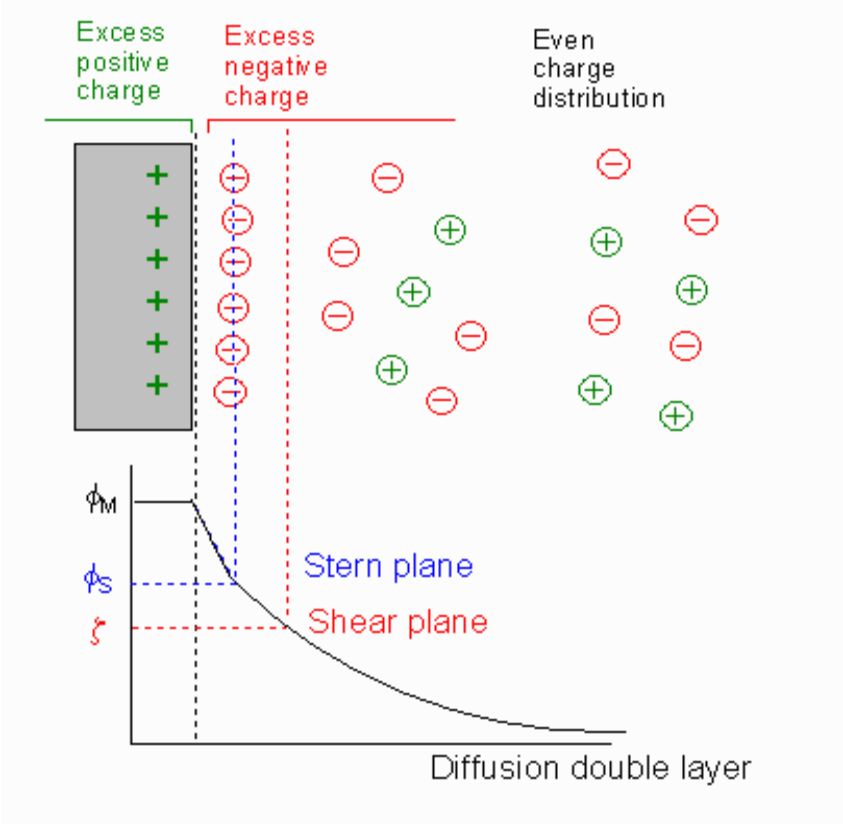

Figure 4: Simplified representation of the double layer and variation of potential from the surface of the current collector [14]

Stern later acknowledged the presence of both the Helmholtz layer and the diffuse layer. According to Stern, there is a compact layer of ions that are adsorbed onto the surface of the current collector. This layer is called the inner Helmholtz layer. There is also another layer of charge that is loosely held onto the surface by columbic forces. This layer is called the outer Helmoltz layer. Beyond the Outer Helmholtz layer, lies the diffuse layer which consists of ions in the solution, whose concentration decreases with distance from the surface of the current collector. Figure 4 also shows the variation of potential with increasing distance from the surface of the current collector. The potential on the metal surface remains constant as the layer closest

to the solution. At this point, we see a steady decrease in potential of the double layer. The potential is at the maximum for the Inner Helmholtz layer. As we move towards the Outer Helmholtz layer, there is a steady drop in potential and the potential is very low for the diffused layer.

There is much more to understand about the electrochemical double layer. The properties of the double layer have variations for different electrochemical systems. In 1957, General Electric first discovered the ability of carbon electrodes to function as an electrochemical double layer capacitor and to store extraordinary amounts of charge [6,15]. Since then, extensive research has been carried out to try and maximize the charge storage characteristics, and to harness the stored energy for useful purposes. One of the main factors that influences the charge storage of the double layer capacitor is the thickness of the double layer system, as described below.

1.4 Pseudo- capacitors

Unlike double layer capacitors, redox supercapacitors store charge due to Faradaic processes. Faradaic process involves transfer of electrons between electrode and electrolyte [16]. Metal oxides and conducting polymers undergo reversible reduction and oxidation reactions (explained below) readily over a potential range [17]. Many conducting polymers and metal oxides are commonly used as electrode materials. Among conducting polymers, polyaniline is a good choice as an electrode material in supercapacitors due to its stability, high conductivity when doped, easy preparation and high specific capacitance [18].

1.4.1 Redox reactions

A reduction-oxidation reaction is one where one of the species present loses electrons, also called ‘oxidised’ while the other species gains the electrons or ‘reduced’.

$$M(s) \rightarrow M^{n+} + ne^{-} \quad (2)$$

$$R^{n+} + ne^{-} \rightarrow R \quad (3)$$

In equation 3 above, *M* loses electrons to achieve n+ oxidation state. Thus *M* is oxidized. On the other hand *R* gains these electrons and becomes reduced. Equations 3 and 4 are called half-cell reactions. The overall reaction for the system would be:

$$M\ s\ + R^{n+} \rightarrow\ M^{n+} + R \quad (4)$$

Formation of rust given below is a common redox reaction.

Oxidation reaction:

$$Fe(s) \rightarrow\ Fe^{2+} + 2e^{-} \quad (5)$$

Reduction reaction:

$$2H_2O\ l\ +\ O_2\ g\ + 4e^{-} \rightarrow 4OH^{-}(aq) \quad (6)$$

The occurrence of reduction and oxidation reactions can be detected by characteristic peaks in the cyclic voltammetry plot of an electrochemical system, as described in figure 5 below.

Figure 5 shows a cyclic voltammetry curve for a purely double layer capacitor and a pseudocapacitor. The curve on the right has peaks at 0.037V and 0.15V. The forward scan has a peak which is the reduction and peak and the current at this point is the peak cathodic current. It is at this point that a chemical species gets reduced to a lower oxidation state. The peak on the

reverse scan is called the oxidation peak and the current at this point is the peak anodic current. Oxidation reaction occurs at this point. The curve on the left is purely double layer and does not display any peaks. The shape of the curve resembles a rectangle.

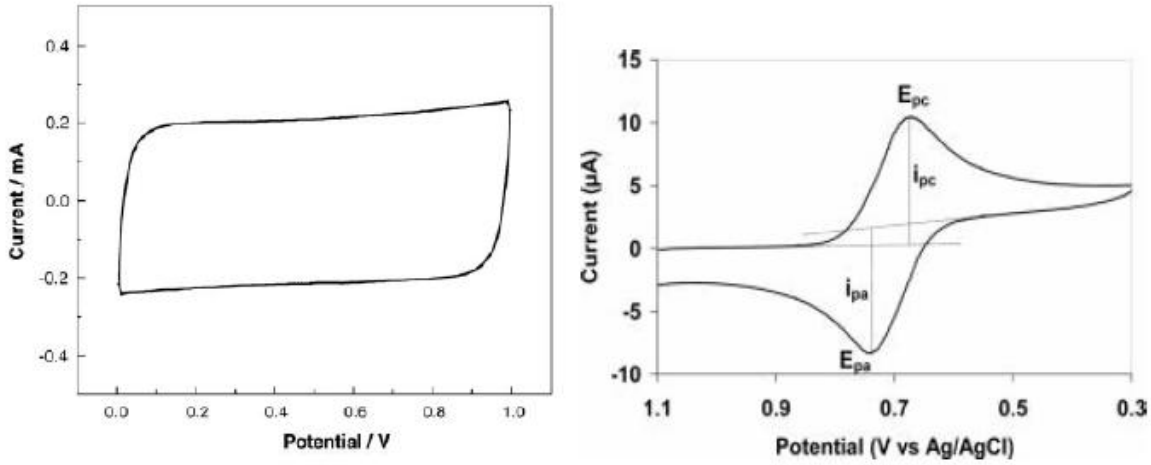

Figure 5: Cyclic voltammetry curve for double layer mechanism (left) and pseudocapacitance mechanism (right) [13]

The electrochemical series lists different elements in the order of their reduction/ oxidation potentials. Elements which are higher up in the series do not get oxidized readily.

1.5 Electroanalytical Techniques

Electroanalytical techniques are commonly used to study and describe the properties of a double layer capacitor. Electrochemical studies are generally performed using a potentiostat or a galvanostat. Common techniques used are electrochemical impedance spectroscopy, cyclic voltammetry and chronopotentionmetry. These techniques give an insight of the thermodynamics and kinetics of the electrochemical reactions, and are described below. Data derived from thee

various techniques, can lead to a better understanding of the formation of the double layer and its properties, and of charge storage and cyclic performance of the systems.

1.5.1 Electrochemical Impedance Spectroscopy

Electrochemical impedance spectroscopy is a powerful nondestructive measurment technique which is used to study the properties of the electrode-electrolyte interface. The technique gives information about the kinetics and mechanics of the reaction. Being an AC technique, the technique is more accurate than DC techniques due to the small excitation amplitude [19]. Impedance spectroscopy technique usually consists of the Bode Plot (impedance vs frequency) and the Nyquist plot (Z' vs Z') which are described below.

In this method, small alternating voltage is applied to a system in steady state, and the response of the system is measured. The system response can be further analyzed with the help of equivalent circuits. The Randle's circuit shown in figure 6 below is commonly used to determine the properties of an electrochemical cell.

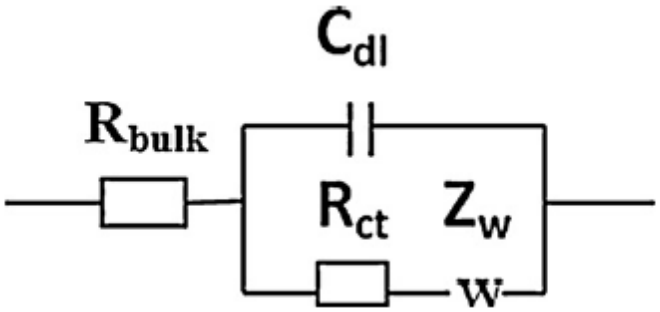

Figure 6: Randle's equivalent circuit [20]

In the above figure, R_{bulk} is the electrolyte resistance and R_{ct} is the charge transfer resistance. C_{dl} is the double layer capacitance and Z_w is called the Warburg element, which is a constant phase element (45° phase).

Solving the Randle's circuit gives us the equation of a circle [12].

$$Z" = (Z' - R_s)/(\omega \times R_{ct} \times C_{dl}) \qquad (7)$$

At the point where Z" is maximum, (Z" = Z' – R_s). Hence

$$\omega_{max} = \frac{1}{R_{ct} \times C_{dl}} \qquad (8)$$

Thus the double layer capacitance of the electrochemical cell can be evaluated at the point where Z" is maximum. Current methodology, allows one to model the equivalent circuit to match the Nyquist plot, allowing for evaluation of associated parameters.

The double layer capacitance in the low frequency region is given by:

$$C = -(\frac{1}{Z'' \omega}) \qquad (9)$$

Figure 7 below represents a typical Nyquist curve which plots Z' (real impedance) vs Z" (imaginary impedance). The plot may vary for different electrochemical systems.

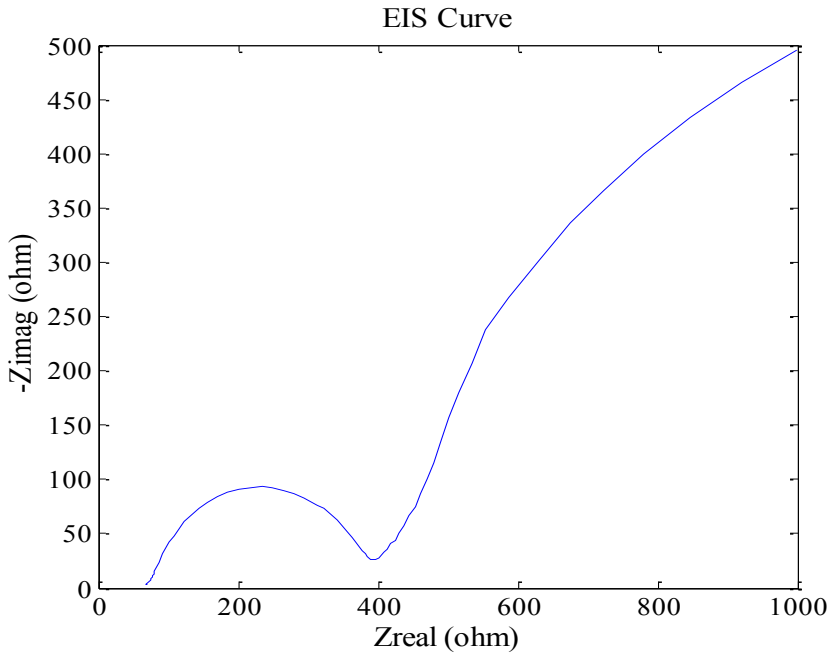

Figure 7: Typical Nyquist Plot

One can see that there is a steady increase in Z" and then the curve starts to change direction. After reaching a minimum value, the curve continues to rise. The semi-circle that is formed corresponds to the formation of the double layer in electrochemical systems. Initially the length of diffusion is very small when compared to the region available for diffusion. When the diffused region and diffusion region become equal, there is a change in direction of the curve. At lower frequencies, there is no longer diffusion and the sharp rise in curve takes place, which corresponds to capacitance component only.

The Nyquist plot provides useful information concerning the properties of the double layer, including the internal resistance and charge transfer resistance of the electrochemical cell. The shape of the curve can also be used to determine electrode properties such as porosity. With an increase in electrolyte penetration depth at lower frequencies a change in the slope of the curve can be observed. This change varies with the pore structure as demonstrated my McDonald et al

[21]. For porous electrodes, we do not see a complete semi – circle. The Warburg curve begins somewhere in-between the semi-circle due to formation of double layer within the pores.

The Bode curve plots the impedance and phase angle as a response to the frequency. Figure 8 is a typical Bode plot. The light blue curve in the figure below shows the change in overall impedance of the cell with frequency and the green curve in the figure below give the change in phase angle with frequency.

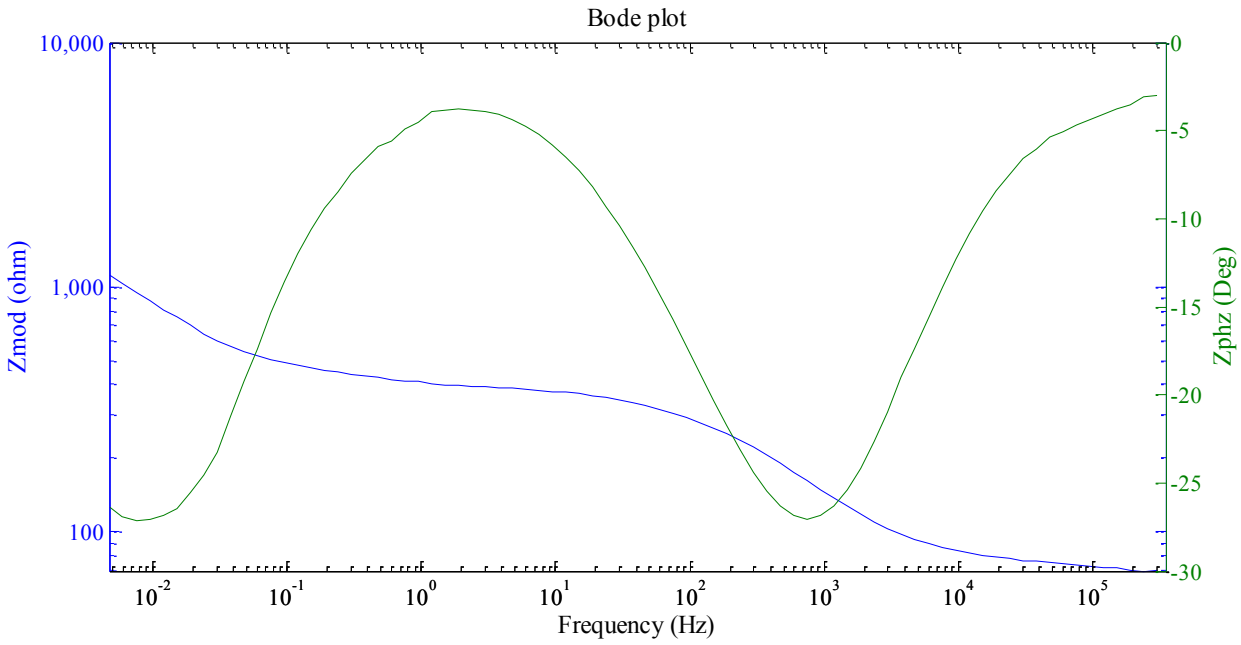

Figure 8: Typical Bode plot

1.5.2 Cyclic Voltammetry

Cyclic voltammetry is an excellent tool to understand the thermodynamics and kinetics of an electrochemical system. In this technique, the current response of the system is measured as a function of step-wise increase/ decrease in voltage. The voltage is applied in the form of a

triangular waveform as shown in figure 9. In cyclic voltammetry, there is a cyclic change in the direction of potential sweep [22], as shown in figure 9.

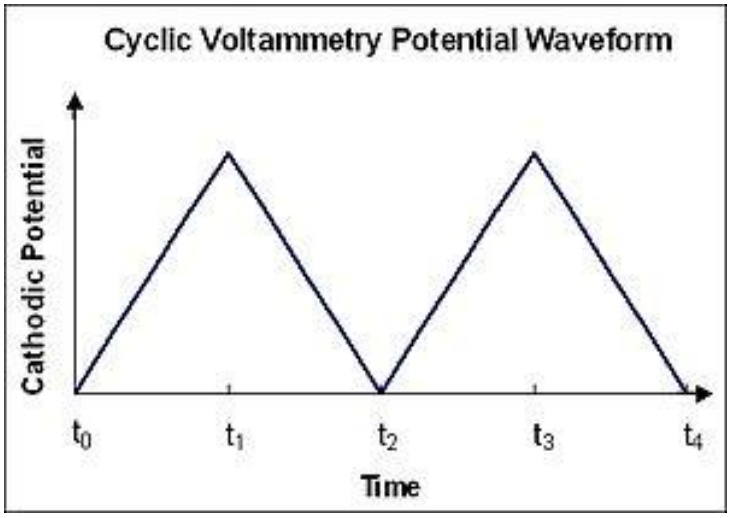

Figure 9: Cyclic voltammetry waveform [23]

The curve is affected by different factors like the scan rate, shape and geometry of the electrodes used.

Figure 10 is an example of how a cyclicvoltammetry for an electrochemical cell with copper ferrocyanide electrodes and 0.1M KOH electrolyte. The current response is plotted on the x-axis and the voltage is plotted on the y-axis. The curve in this case is for one complete sweep between 0.5 and -0.5 volts.

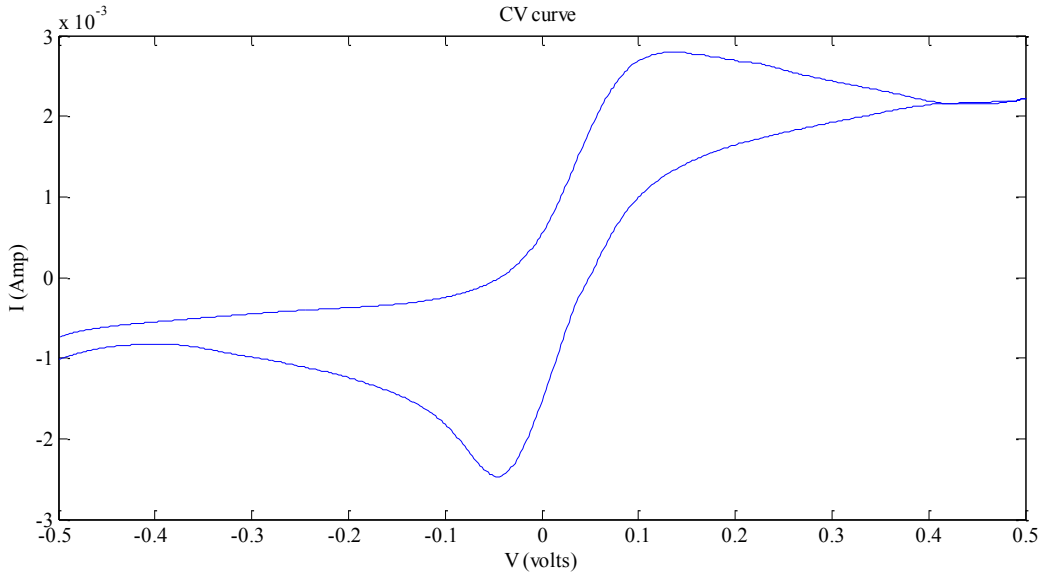

Figure 10: Cyclic voltammetry curve of copper ferrocyanide electrodes

The total charge stored is measured by calculating the total area within the curve. Capacitance is given by:

$$Q = C/V \qquad (10)$$

Where Q is the total charge and V is the voltage across which the cell is swept.

The total energy stored is given by:

$$E = \frac{1}{2} .C.V^2 \qquad (11)$$

Where E is the total energy stored, C is the capacitance and V is the applied voltage range.

The two peaks in figure 10 correspond to reduction and oxidation reactions that take place in the system. The presence of peaks indicates that a redox supercapcitor is formed in the system. For a purely double layer supercapacitor, the curve will closely resemble a rectangle. The peak currents and peak voltages are usually determined with reference to a zero current baseline. The curve is dependent on the scan rate of the system. At low scan rates the system is diffusion controlled and not much information can be obtained regarding the kinetics of the reaction. At faster scan rates there is some thermodynamic control as well [12].

The curve usually shifts during the initial cycles before becoming repetitive. The system does not stabilize immediately, hence resulting usually in a shift in the curve. Cyclic voltammetry is usually performed over many cycles to determine the time that the system takes to stabilize and to see how long it can maintain its stable performance.

1.5.3 Chronopotentiometry

Chromopotentiometry is an electroanalytical technique commonly used to study the cycling life of energy storage systems and devices, and to evaluate their energy and power densities. In this measurement technique, the electrochemical system is alternately charged and discharged and the change in potential is measured as a function of time.

Figure 11 below shows the chronopotentiometry curve for a polyaniline-carbon composite at 4mA current. The cell is first charged to a peak voltage value of 0.2V. Following this, the cell is discharged by applying the same current in the opposite direction. During both processes, the change in voltage is measured as a function of time. The energy and power density of the cell during discharge can be calculated using this data.

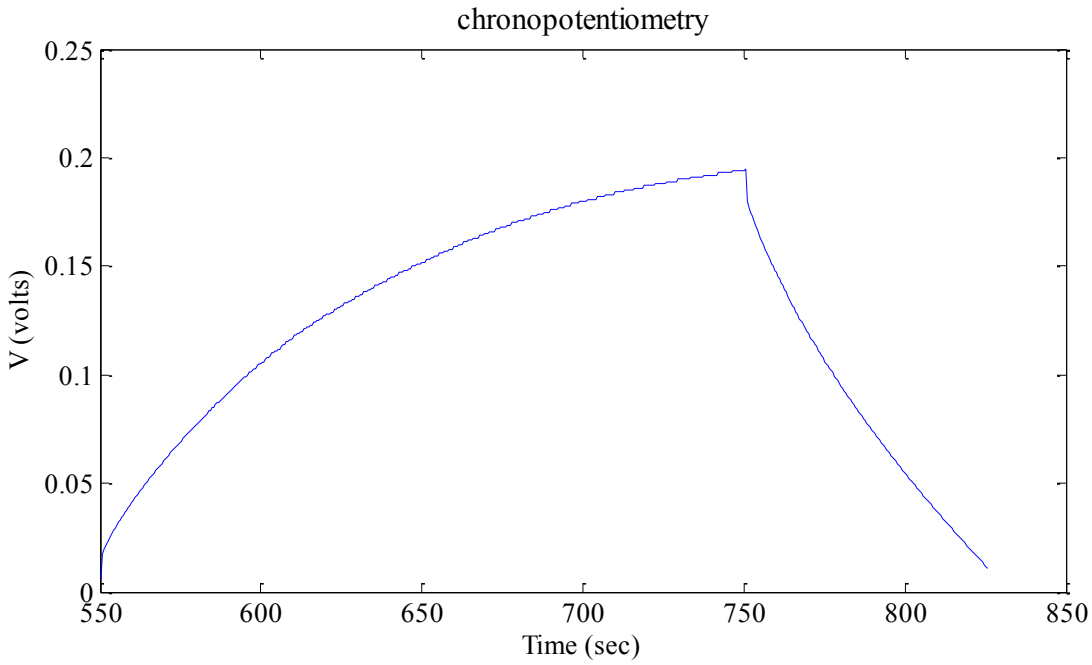

Figure 11: Chronopotentiometry curve for polyaniline – carbon composite

The chronopotentiometry curve during discharge has two distinct components. A sudden initial drop in voltage due to the internal resistance is noticed. This is followed by a curve with due to the capacitive component [24].

The specific capacitance is given by:

$$C_m = \frac{i \times t}{\Delta V \times m} \qquad (12)$$

Where,

Cm = specific capacitance (F/g)

i = charging/ discharging current (mA)

t = time of charging/ discharging (sec)

ΔV = change in voltage (mV)

m = mass of electrodes (g)

The energy density is given by:

$$E = (\frac{1}{2}) \times C_m \times \Delta V^2 \qquad (13)$$

The power density is given by:

$$P = \frac{i \times \Delta V}{2 \times m} \qquad (14)$$

Similar to cyclic voltammetry, chronopotentiometry tests are performed to study the cyclic behavior of supercapacitors. A good supercapacitor would have discharge characteristics that are repeatable over a long period of time. Supercpacitors with short discharge times will have very low energy density. The energy and power densities measured using chronopotentiometry give us a better idea of what the actual output of the supercapacitor would be.

The above described techniques have been used by researchers to understand the behavior of various energy storage devices. These techniques have been used extensively in this work to better understand conductive polymer composite based supercapacitors.

1.6 Conductive polymer composites [25]

Conducting polymer composites are typically formed with an insulating polymer matrix and a conductive filler material that can make the overall composite highly conductive, depending on filler concentration. At low concentrations of filler material, the distance between adjacent particles is relatively large and hence the conductivity of the system is fairly low. With increasing filler addition, electrons are able to travel from one particle to another, thereby increasing the conductivity of the system. At a critical threshold value, a continuous conductive domain is created throughout the composite. At this point a sharp decrease in resistivity is typically observed.

In figure 12 below, one can see a rapid rise in conductivity of the composite at the critical volume (V_c). There is no significant rise in conductivity beyond this point. An increase in dielectric property of the system is also concurrently observed [26].

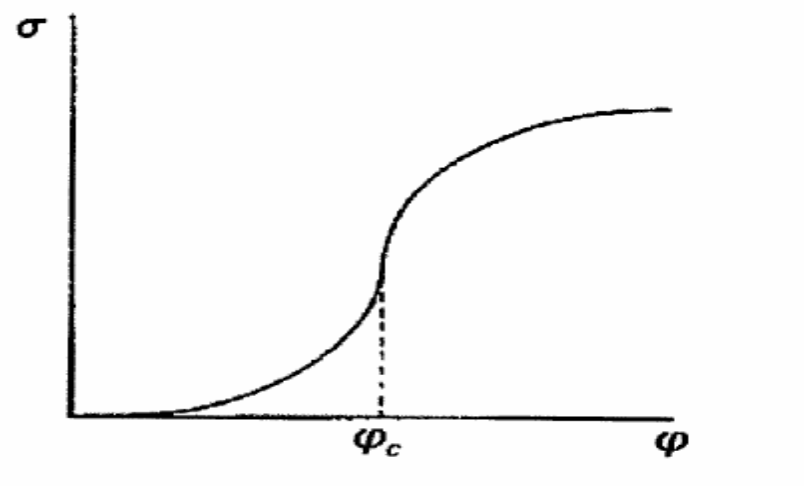

Figure 12: Percolation behavior in a conductor – insulator system [26,27]

In this work, the approach used was to take advantage of this percolation phenomenon and use the composites prepared by the same methodology as electrodes in a supercapacitor system. ABS – graphite (conducting polymer composites) was compared to PANI – graphite/ activated carbon composites to understand the capacitance properties.

1.7 Current Work

The ability of supercapacitors to store a large amount of charge has created a high level of interest in this field. In recent published works, much interest has been shown in incorporating high surface area carbon materials in supercapacitor electrode systems. Doping the carbon materials with active species like conducting polymers, which have high oxidation and reduction rates results in pseudo-capacitors with high specific capacitance.

Balagun et al. [26] has done extensive research on acrylonitrile butadiene styrene – graphite composites. Their study indicates that the composite exhibits percolation behavior, which results in a sharp increase in conductivity of the material. The authors primarily developed a partial solubility mixing techniques, which bring down the percolation concentration. The study also shows us that the materials exhibit good strength and is wear resistant. The latter property assures that the material will remain stable in an electrochemical cell component.

Wei-Chih Chen et al**.** [17] have demonstrated that by implanting polyaniline on high surface area carbon using cyclic voltammetry, a significant increase in specific capacitance can be achieved. The specific capacitance went up to 180 F/g in the case of the composite as compared to 92 F/g for the carbon electrodes. This increase in capacitance has been credited to pseudo-capacitance due to the presence of polyaniline.

Wang Qin et al. [18] have also investigated the effect on the specific capacitance of loading polyaniline on activated carbon. Their results also indicate an increase in specific capacitance after doping with polyaniline, which can be attributed to pseudo capacitance coupled with double layer capacitance. Pure polyaniline electrode showed a 36% decrease in capacitance over fifty cylces while the capacitance for polyaniline-activated carbon composite electrodes decreased by 7%. The composite electrode has better cyclic stability compared to pure polyaniline electrode.

Tripathi et al. [28] have used electrochemical impedance spectroscopy to study the performance of conducting polymer electrodes based supecapacitors that use polymeric gel electrolytes. They reported the capacitance in terms of the surface area of the electrode (mF/cm2) along with specific capacitance.

Arora et al. [11] have done extensive investigation on the role of separators and defined the properties of an ideal separator. Some of the key properties highlighted are: low ionic resistance, good mechanical and chemical stability and uniform thickness. There was no one separator that exhibited all the required properties so a compromise was made based on the needs.

1.8 Motivation

The need for a large energy storage device to replace conventional batteries has been the main driving cause for a much research on supercpacitors. These devices exhibits high power densities and very high recyclability (can be charged for a large number of cycles without much decrease in charge storage), which make them environmentally friendly. Although advancements have been made, the many disadvantages of these devices have offset their regular use. There is a large amount of literature that has addressed some of the critical issues and has constantly reported increasing energy storage and energy density. Hence, there is a realistic possibility of

them replacing conventional batteries at some point; the negative issues can be adequately resolved. The desire to contribute to solving these existing issues has inspired this work on conductive polymer composite supercapacitors.

1.9 Objectives

The primary objective of this work was to develop an electrochemical cell that would help to isolate the variables that govern charge storage. Plastic leur lock syringes were chosen to develop the electrochemical cell. The syringes helped to maintain vacuum within the cell body and were also cost effective. The next objective was to study the performance of conductive polymer composite electrodes as a double layer capacitor and the role of percolation on the capacitance. For this objective acrylonitrile butadiene styrene was chosen as the polymer material and graphite (surface area: 115 m^2/g) was chosen as the filler material. Prior work had been done to understand the properties of this composite and it was chosen due to the good conductivity it showed at the percolation threshold and its mechanical properties.

The third objective of this research was to compare the performance of the double layer capacitor with that of a pseudo-capacitor. To go about this, composites of conductive polyaniline were formed with different high surface area carbon materials. This composite was chosen because the presence of polyaniline improves the capacitance and the system has better cycling stability as compared to pure polyaniline.

The fourth objective was to understand the use of copper ferrocyanide as an electrode in supercapacitors. The complex material was prepared in the laboratory and was tested in the electrochemical cell under different conditions.

The final objective was to study the effect of some of the governing factors (separator material, electrode surface area, electrolyte and distance of separation) on the overall charge storage.

To accomplish these goals, the electrode was prepared in the form of a 1 inch diameter pellet and was incorporated in the electrochemical cell along with suitable electrolyte and separator.

EXPERIMENTAL

2.1 Materials

2.1.1 Acrylonitrile butadiene styrene (ABS)

ABS is a thermoplastic and a copolymer that is prepared by polymerizing acrylonitrile and styrene in the presence of polybutadiene. The polymer used in my experiments is called ABS – 40 (40% acrylonitrile, 45% butadiene and 15% styrene). ABS – 40 was obtained from Sigma – Aldrich. At temperatures above 80^0C, the polymer starts to flow [26]. Table 1 illustrates some key properties of 'as received' polymer. Figure 13 below shows the monomer units of ABS.

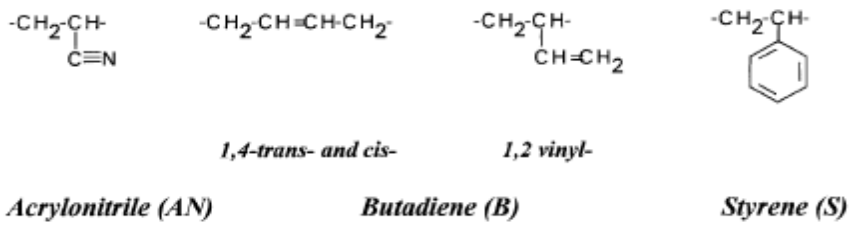

Figure 13: Monomers of ABS [29]

Table 1: Properties of ABS -40 polymer

Properties	ABS -40
Denisty at 25^0C (g/cm3)	1.04
Flow Temperature	80^0C
Particle Size (μm)	<1100

2.1.2 Polyaniline

Polyaniline used in the experiments is obtained in form from Sigma – Aldrich. The conducting polyaniline is in the form of conductive emaraldine salt and has a green appearance. Table 2 tells us the essential physical and chemical properties of 'as received' polyaniline. Figure 14 below shows the chemical formula of polyaniline.

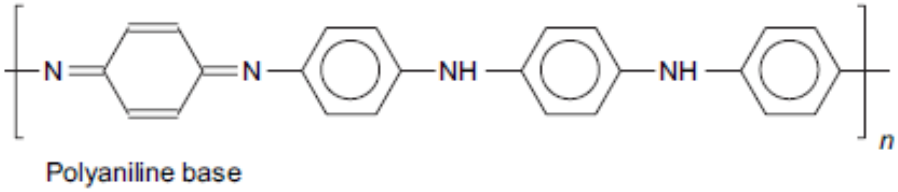

Polyaniline base

Figure 14: Polyaniline chemical formula [30]

Table 2: Properties of conducting and non – conducting polyanilne

Properties	**Conductive Polyaniline**
Color	Green
Density at 25^0C	1.36 g/ml
Conductivity	2-4 S/m
Average Molecular Weight	>15000
Particle Size	3-100 µm
Surface Area	5-20 m2/g

2.1.3 Graphite and activated carbon

The graphite and activated carbon used for the experiments are obtained from Asbury Graphite Mills Inc. Table 3 below gives the surface area and pore volume of graphite and activated carbon.

Table 3: Properties of graphite and activated carbon

Properties	Synthetic Graphite	Activated Carbon
Surface Area (m^2/g)	115	900
Pore volume (cc/g)	-	0.80

2.1.4 Copper ferrocyanide

The copper ferrocyanide used as electrodes was prepared in the lab. Two moles of copper sulfate is mixed with one mole of potassium ferrocyanide stoichiometrically.

$$2\,CuSO_4 + K_4\,Fe\,CN_{\,6} \rightarrow Cu_2\,Fe\,CN_{\,6} + 2\,K_2SO_4 \qquad (15)$$

The solution is made slightly acidic by adding a drop of concentrated sulfuric acid to 50 ml of copper sulfate solution. Copper sulfate is added in excess to avoid any residual potassium ferrocyanide from mixing copper ferrocyanide. The copper ferrocyanide is obtained by centrifuging the mixture and rinsing with distilled water. The residue is the allowed to dry in an oven at 80^0 C for 24 hours. The copper ferrocyanide obtained is dark brown in color.

2.1.5 Conductive carbon tape and tabs

Conductive carbon tape and tabs, used to attach the electrode to the current collector are obtained from Electron Microscopy Sciences. These are two side sticky scanning electron microscopy grade tabs.

2.2 Preparation of composite [26]

The composite is prepared using a special technique developed previously in the lab. The polymer and filler materials are weighed out in the required proportion. The filler material is first mixed with a solution of 10% acetone and 90% isopropyl alcohol in a ratio of 1:3. This mixture is stirred thoroughly for five minutes using a magnetic stirrer. The polymer is then added to the mixture. The polymer – filler mixture is then milled at a rate of 120 rpm for 10 minutes in a horizontal mill. The composite is then filtered using vacuum filtration technique and the residue is kept in an oven at 40^0 C for a period of 24 hours.

2.3 Die pressing

The die pressing equipment was a 3912 model obtained from Carver Laboratory Equipment. Figure 15 show the Carver press used to press composite samples. 0.8 g of the composite was weighed and pressed in a 1 inch die. In the case of ABS samples, a pressure of 120 MPa is applied and the pressing technique used was hot pressing. Figure 16 shows the composites that were pressed. The sample is heated to a temperature of 100^0 C or 130^0 C and then allowed to cool down to room temperature. In the case of PANI composite, the sample is pressed without any heat at 130MPa for about 1minute.

Figure 15: Carver Laboratory equipment Model 3192 Die Press

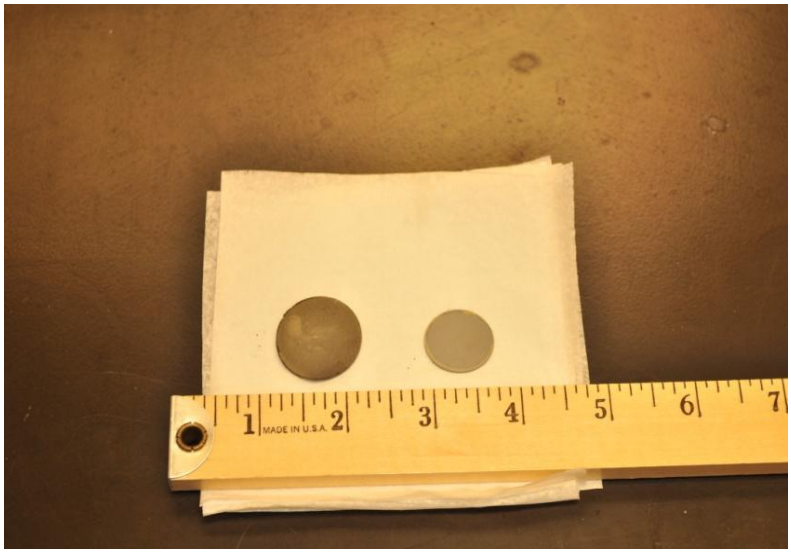

Figure 16: Composite pellets pressed on the die press

2.4 Electrochemical cells

2.4.1 Two electrode cell

A two electrode cell was developed within the laboratory. Figure 17 shows a schematic representation of the two electrode cell. The cell is constructed using 50 cc plastic Leur Lock syringes obtained from Fischer Scientific. Silver and copper discs obtained from Jatayu Jewellers (San Diego, CA) were used as current collectors and were attached to the end of the syringe plunger using o-rings and superglue. Figure 18 shows the actual cell developed in the laboratory. Copper wires attached to the current collectors are used as leads for the electrochemical cell. The plungers helped to maintain a vacuum within the cell. A small sealable orifice was used for adding electrolyte. The electrodes which are in the form of pellets are attached to the current collectors using conductive carbon tape obtained from Electron Microscopy Sciences. Electrodes are also coated directly onto the surface of the current collector in order to obtain a thin coating. The electrochemical cell was mainly used to determine actual cell capacitance. Keeping the general environmental challenges in mind, the cell is also reusable.

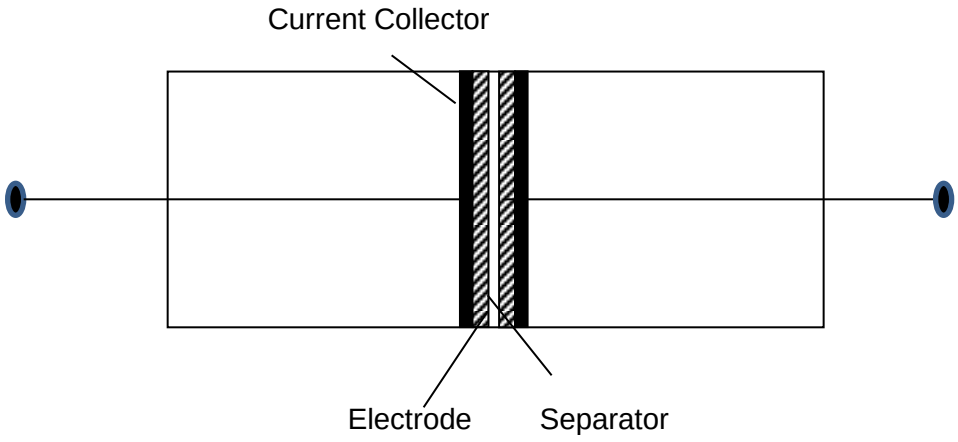

Figure 17: Schematic representation of the electrochemical cell

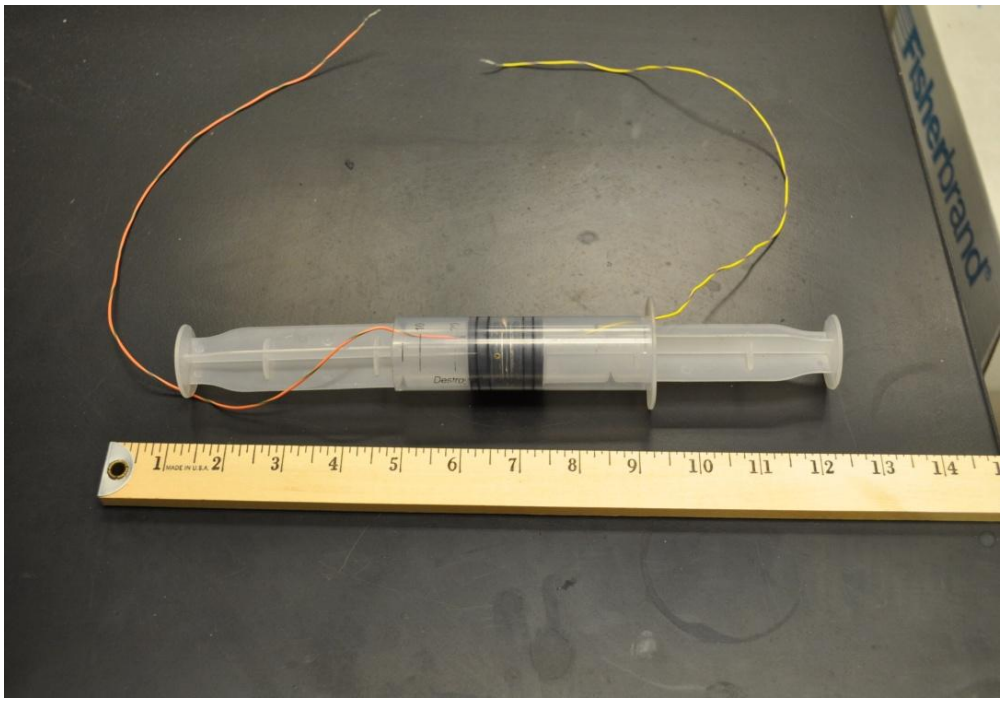

Figure 18: Electrochemical cell developed in lab

2.4.2 Three electrode cell

The three electrode cell used in the experiments is a standard electrochemical flat cell. Figure 19(a) shows a schematic representation of a three electrode cell. The reference electrode has a known potential and is used to control the potential of the working electrode while the counter electrode is required to carry the current flowing through the circuit. Figure 19 (b) shows the actual cell used to make measurements. In this cell the counter electrode used is platinum and the reference electrode is standard calomel electrode. The working electrode consists of the composite pellet attached to the silver disc (current collector), using a carbon tape, or a thin layer of the composite coated onto the surface of the silver disc as bonding agent. Use of the three

electrode cells provided copious data and detail about the capacitive properties of the composite materials.

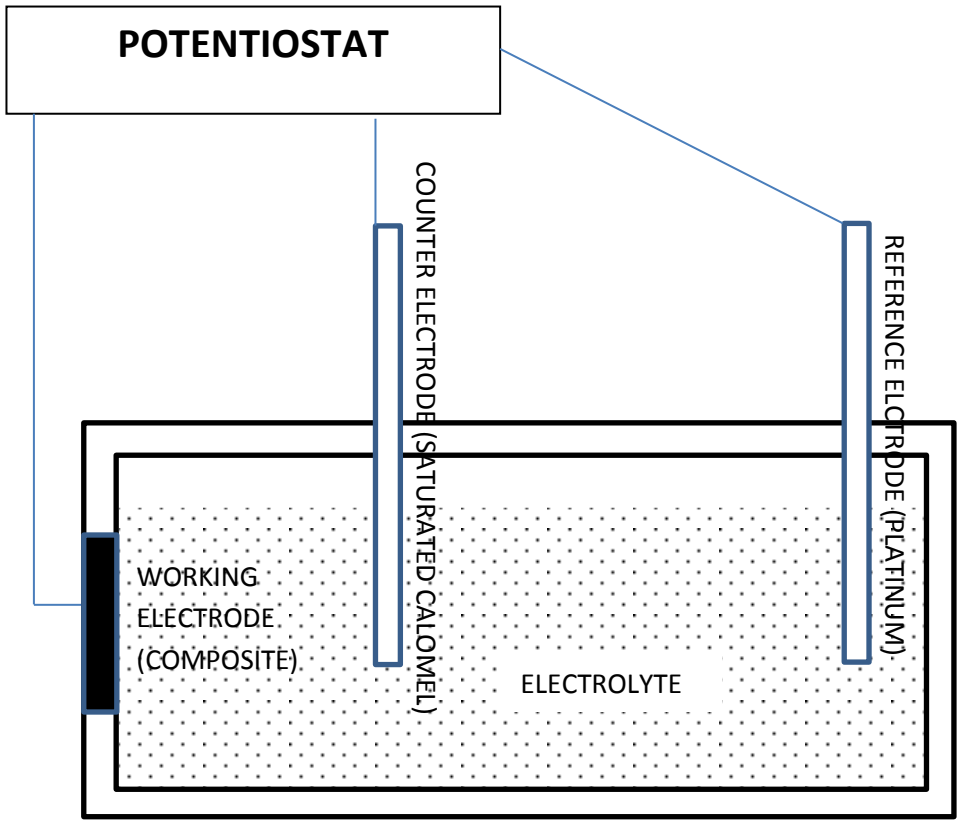

Figure 19(a): Schematic representation of a three electrode cell

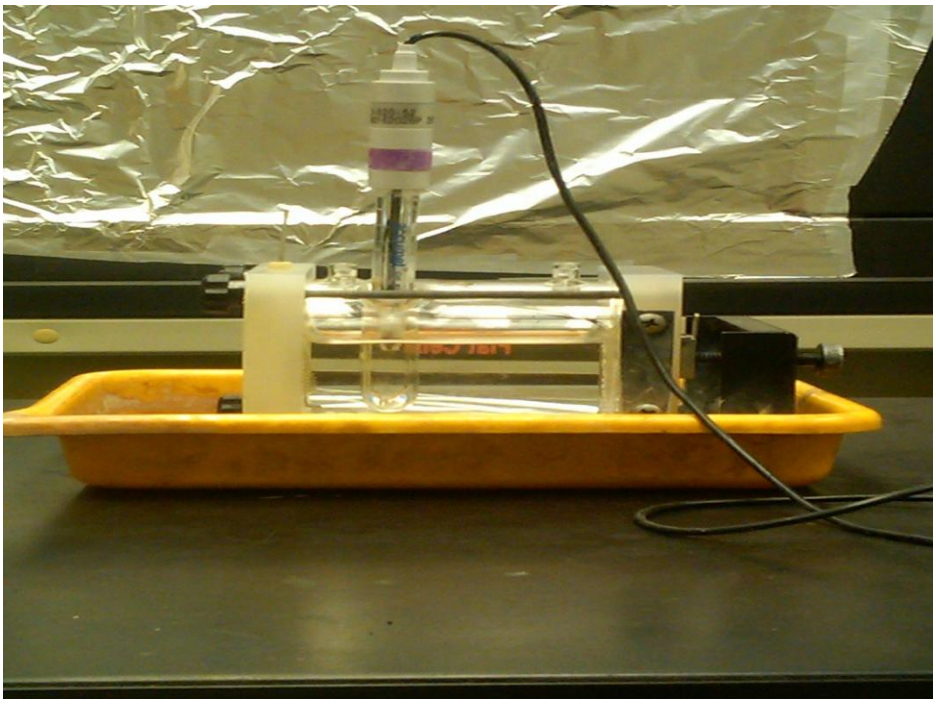

Figure 19 (b): Electrochemical cell used in measurements

2.5 Electrochemical characterization

All electrochemical characterizations were performed using a series G-300 potentiostat obtained from Gamry Frameworks. The potentiostat aids in performing electrochemical impedance spectroscopy, cyclic voltammetry and chronopotentiometry tests.

2.5.1 Electrochemical impedance spectroscopy

The electrochemical impedance spectroscopy test is a technique used to understand the properties of the electrochemical double layer that is formed. All tests were performed at 0.75V with alternating pulses of 5mV at varying frequencies. The electrochemical cell was allowed to stabilize for a period of thirty minutes before the test. The resultant nyquist curve plots imaginary impeadnace versus real impedance and bode curve plots impedance and phase angle as functions of frequency.

2.5.2 Cyclic voltammetry

The cyclic voltammetry test gives us a better understanding of the energy storage properties of the electrochemical cell. The charge storage mechanism can be determined using this test. Since electrolytes used in the tests are aqueous, a voltage of 1.2 V represented the voltage limit, in order to avoid electrolysis of the solution. All tests were run between -0.5 – 0.5 V or between -0.2 – 0.8V. The cyclic voltammetry test is run immediately after the electrochemical impedance spectroscopy tests.

2.5.3 Chronopotentiometry

The chronopotentiometry test gives us data about the charging and discharging properties of the electrochemical cell. One can determine the actual capacitance of the cell when it is discharging and the energy and power density of the cell can also be determined. The chronopotentiometry tests are carried out at 4mA and 6mA charging/ discharging currents. The electrochemical cell is charged/ discharged at a constant current and the change in potential is measured. The resultant curve provides data about the change in capacitance with current density.

2.5.4 Echem analyst

Echem Analyst is the analysis software from Gamry frameworks. All the test data obtained are analyzed using this software. The software facilitates the measurement of area under the cyclic voltammetry curve.

2.6 Physical characterization

2.6.1 Scanning electron microscope

The surface properties of electrodes were analyzed using a scanning electron microscope. Polyaniline samples were highly conducting and surface was viewed without polishing. The polymer-filler matrix of ABS composites was viewed for polished cross-sections. All scanning electron microscope analysis was done in the secondary electron mode.

2.6.2 Energy dispersive spectroscopy

Energy Dispersive Spectroscopy technique was used to characterize copper ferrocyanide electrodes. This technique gives us information of impurities present and also element distribution over the surface. This technique analyses the x-rays generated from a sample bombarded with electrons.

2.6.3 X-ray diffraction

X-ray diffraction ware used to characterize the composites and copper ferrocyanide samples to study the phases present, crystallinity and chemical composition of the samples. Diffracted x-rays are produced, from a sample subjected to monochromatic x-rays, when Bragg's law is satisfied. These diffracted x-rays are analyzed to determine the phases present and crystallinity of the sample.

RESULTS & DISCUSSION

3.1 Calibration with silver disc electrodes

The cell was initially calibrated using silver discs as electrodes .The silver discs were later used as current collectors, when experiments were performed with ceramic and conductive polymer composite electrodes. These tests were primarily performed to provide data on the workings of the electrochemical cell, and to determine the extent to which silver discs contribute to the overall capacitance measured for the composites. The silver discs were of diameter of 1 inch, and were polished thoroughly to obtain a clean surface. The electrochemical cell capacitances were calculated under dry and wet conditions with a filter paper separator. Table 4 below gives us the cell capacitance and capacitance as a function of area. The capacitance values reported here are calculated from CV curves of the respective electrochemical cells.

Table 4: Capacitance data for silver disc electrode supercapacitors

Cell Condition	**Capacitance (mF)**	**Capacitance as a function of area (mF/cm^2)**
Dry	1.43×10^{-3}	2.82×10^{-4}
Wet (0.1 M KOH)	9.5	1.87
Wet (1M H_2SO_4)	650	64.22

We can see from Table 4 that the overall capacitance of the cell is very low. There is an improvement in capacitance upon addition of electrolyte. Under dry condition, the cell behaves

like a regular capacitor while the addition of electrolyte results in the formation of double layer and an increase in capacitance. The cell capacitance is still pretty low.

.The low capacitance values obtained were a result of very low surface area available to form a double layer. Use of aqueous electrolyte, limits the testing to a lower voltage range of lesser than 1.2V [31]. Above this voltage, electrolyzing of water affects the validity of the signals. Thus all tests are performed within this limit.

3.2 Electrochemical measurements of ABS – graphite composite

3.2.1 XRD analysis of ABS – 8 % graphite system

Figure 20 shows the x-ray diffraction study of ABS-8% graphite composite. The big hump at 20^0 and the sharp peak at about 26^0 coincide with the characteristic peaks of ABS 40 and synthetic graphite respectively **[26].** The fact that the peaks have not shifted in the composite would indicate no reaction between the graphite and ABS in the composite.

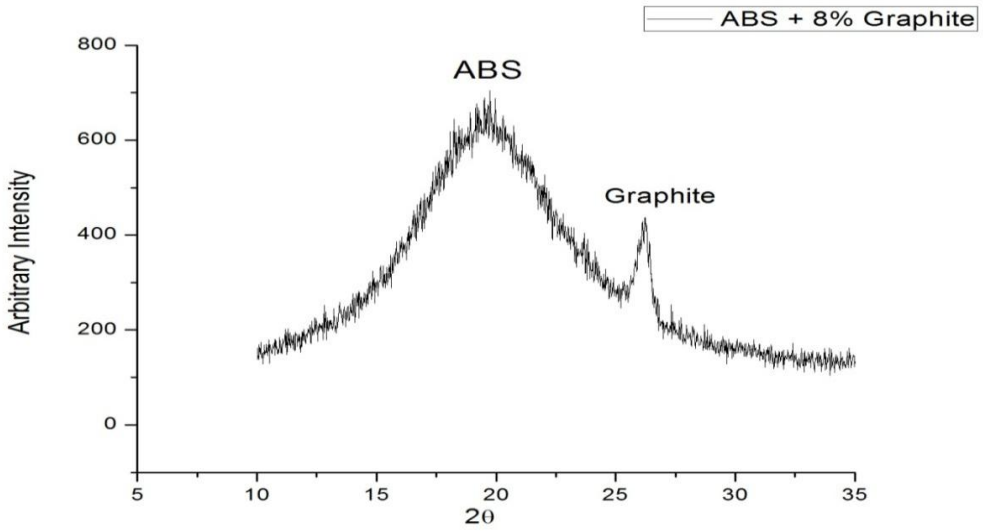

Figure 20: XRD analysis of ABS – 8% graphite sample

3.2.2 Bode plots for ABS-graphite composites

Figure 21 above show Bode plots for the ABS – graphite composites that were used as electrodes in the electrochemical cell. The plots show the change in impedance and phase angle with frequency of ABS- graphite composites with varying graphite content.

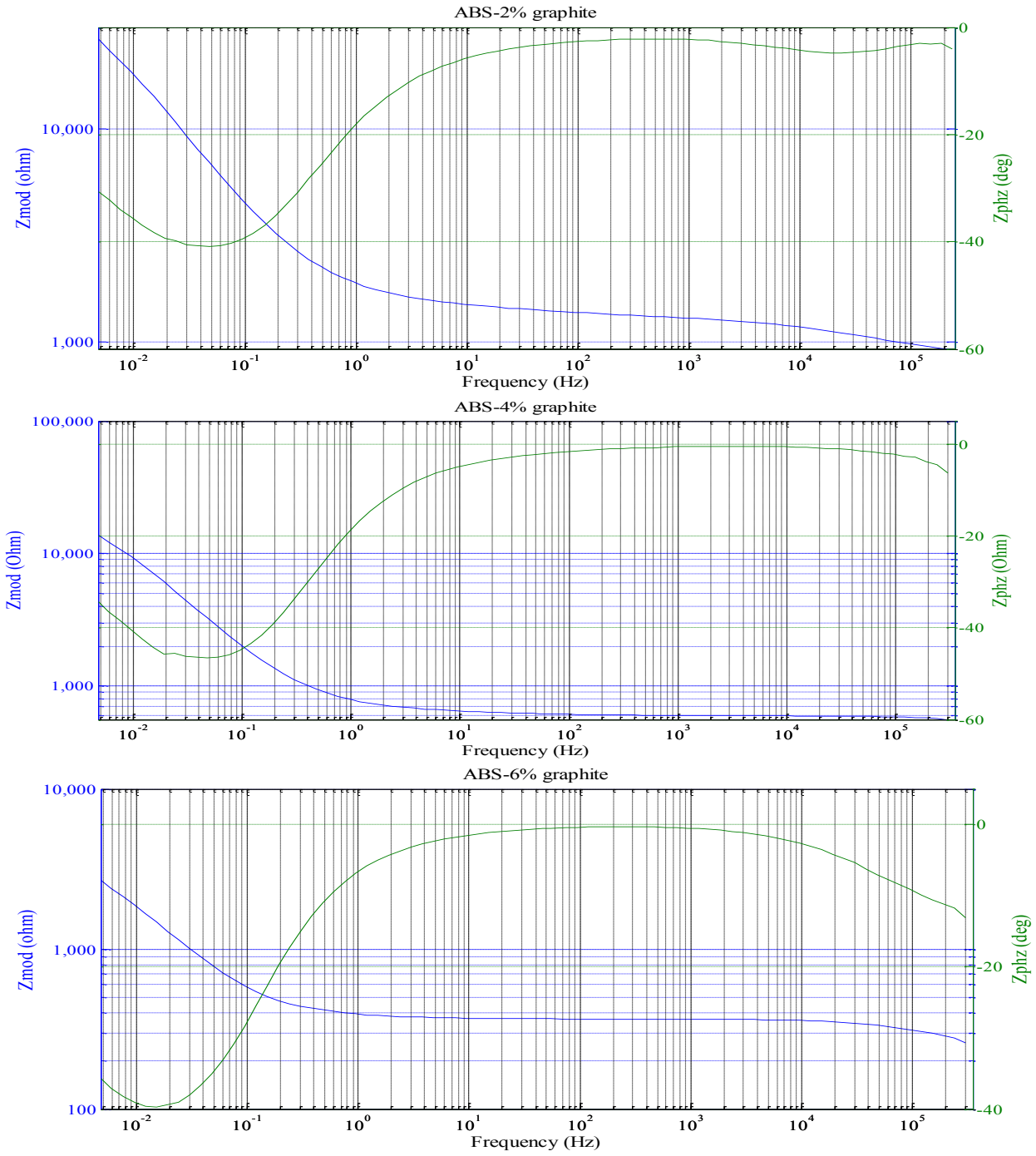

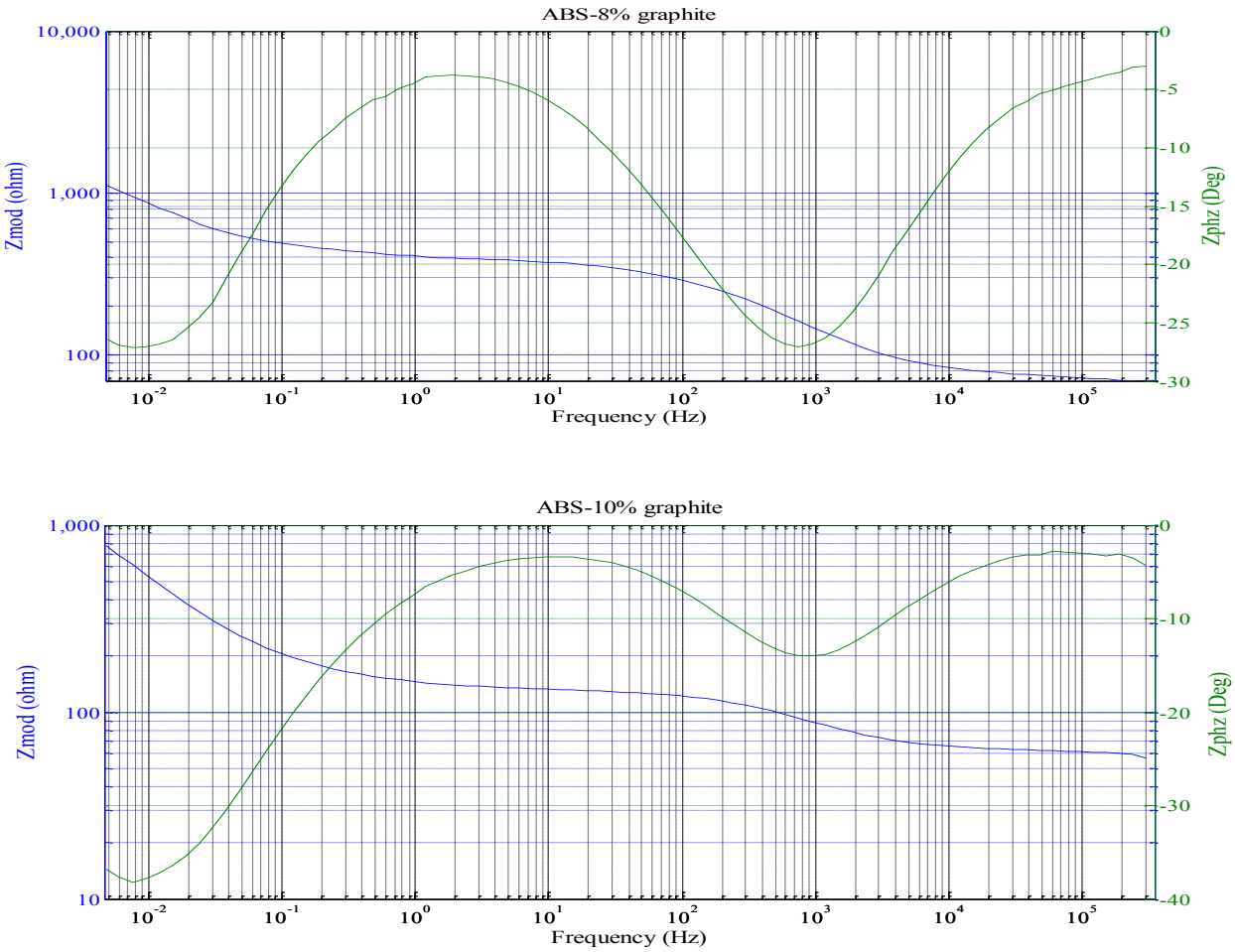

Figure 21: Bode plots for ABS – graphite composites (2, 4, 6, 8, and 10%)

Typically, the composites have both capacitive and resistive nature. In the high frequency region, the impedance versus frequency curve has a zero slope. In this region, the impedance is not dependent on frequency and the cell is resistive in nature. At the lower frequency region, the slope of the impedance versus frequency curve is around -1 [32]. It is in this region that the cell displays capacitive behavior. This region corresponds to phase angles between 0^0 and 30^0. ABS - 8, 10% graphite composites display capacitive behavior in the higher frequency region as well.

3.2.3 Capacitance based on percolation theory

Composite of ABS polymer and conductive graphite (surface area: 115 m^2/g) was prepared with varying weight percentage of graphite. The composites were then pressed into pellets of 1 inch diameter, each weighing 0.8g. These pellets were then incorporated in the two electrode cell design. Electrochemical impedance spectroscopy and cyclic voltammetry tests were performed on this setup. The electrolyte used was 0.1 M KOH. The electrochemical impedance spectroscopy tests were performed between 300,000 Hz and 0.005 Hz frequency at voltage of 0.75V.

Table 5 below presents EIS data on these samples. The capacitance was calculated at the lowest frequency. A steady increase in capacitance was seen with increase in graphite content. The corresponding EIS curves are shown in figures 22 (a) and (b) respectively.

Table 5: Calculated capacitance and specific capacitance for different graphite quantities (EIS)

Graphite weight %	Capacitance value (mF)	Specific Capacitance (mF/g)
2	3	1.875
4	6	3.75
6	20	12.5
8	65	40.625
10	69	43.125

Figures 22(a) and 22(b) show the EIS curves for the composite at different graphite percentages. The EIs curves plot the real part of impedance versus the imaginary part of impedance. One sees

that with increase in graphite content, the electrochemical double layer forms much faster. There is a consistent drop in the impedance of system. This can be attributed to the increase in conductivity of the system with addition of graphite.

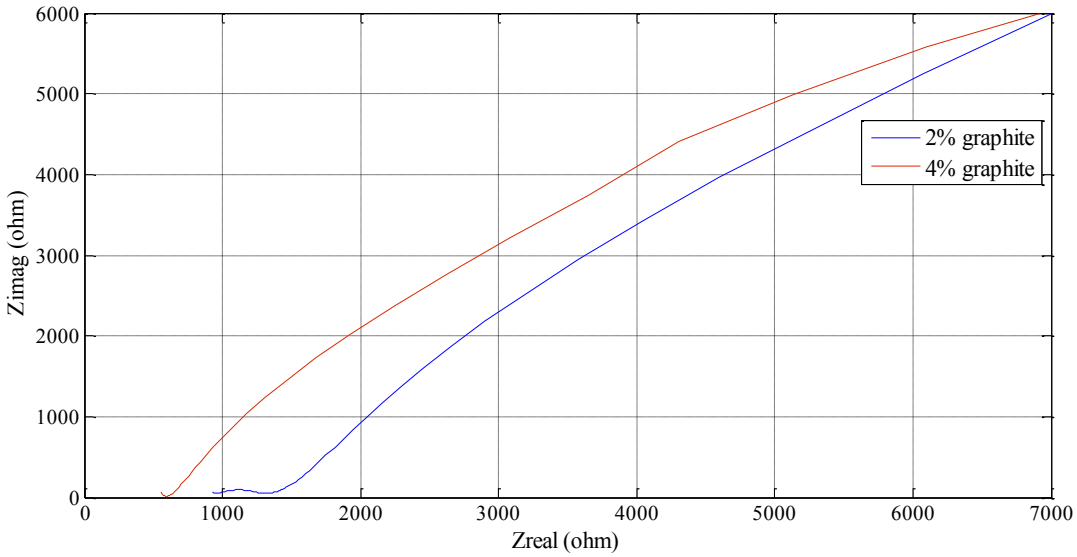

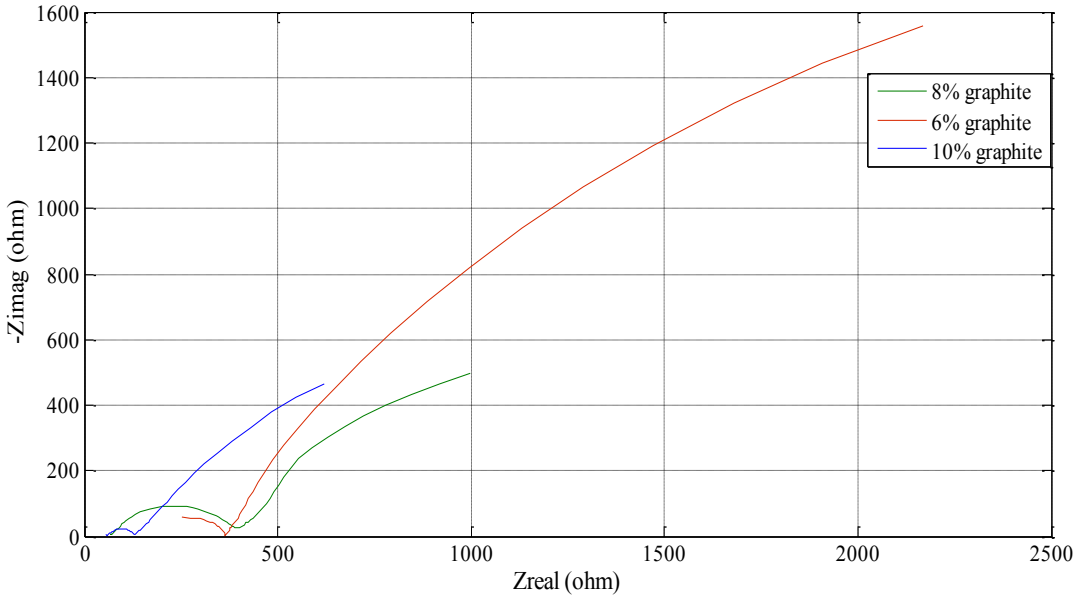

Figure 22(a) and 22(b): EIS measurements for ABS doped graphite (2, 4, 6, 8 and 10%)

Figure 23 shows us the variation of capacitance with graphite present in the composite. A sharp rise in capacitance from 6% to 8% was noticed before the curve flattens again. This phenomenon can be attributed to the percolation behavior of ABS – graphite system. The graphite gets deposited on the ABS grain boundaries of the composite and there is a certain threshold value where conductive domains are setup which results in continuous conductive domains and an overall rise in conductivity of the composite. With increase in conductivity of the electrode, more ions are attracted to the surface. With a sudden jump in conductivity at percolation threshold, a sharp rise in capacitance was hence observed. The vertical nature of the Warburg curve shows the capacitive nature of the electrochemical cells.

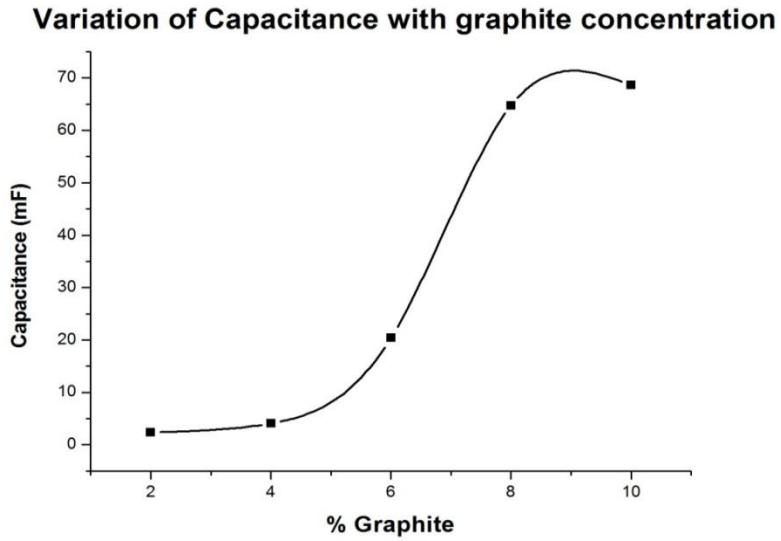

Figure 23: Variation of capacitance with graphite content (EIS)

Table 6 gives the bulk and charge transfer resistance for the five different composites. Figure 24 shows us how the bulk and charge transfer resistances are calculated from an EIS curve. The bulk resistance of the ABS – graphite system decreases with increase in graphite content.

Table 6: Bulk and charge transfer resistance for ABS – graphite composites

Composite	Bulk Resistance (ohm)	Charge transfer resistance (ohm)
ABS -2% graphite	912.4	399.6
ABS -4% graphite	510.4	88.2
ABS -6% graphite	134.2	223.2
ABS -8% graphite	69	326.5
ABS -10% graphite	61.74	69.06

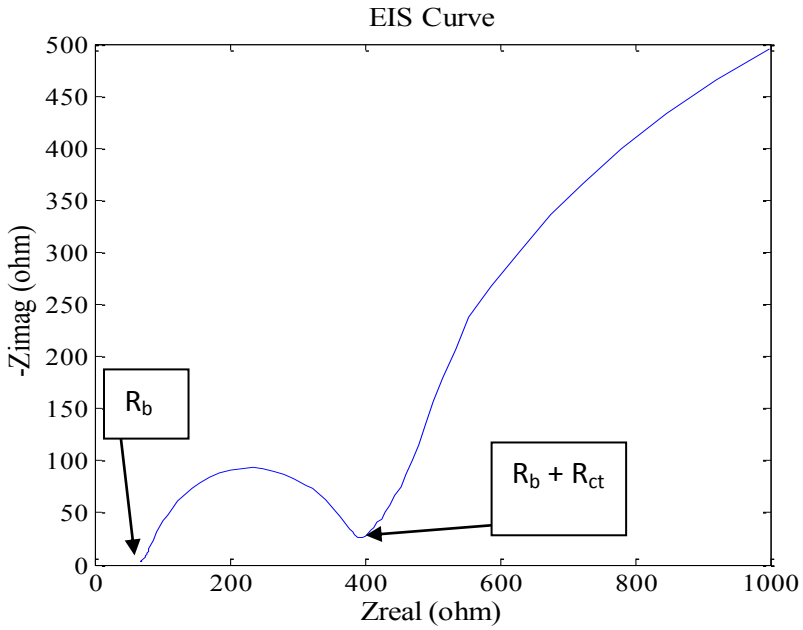

Figure 24: Calculation of bulk and charge transfer resistance

Table 7 gives the capacitance data calculated from the CV curves for the composites. There was a steady rise in capacitance with increasing graphite content. Cyclic voltammetry tests were conducted for the samples between 0 - 1 V. These tests were performed immediately after the

EIS measurements. Four cycles were performed and the capacitance was measured at the third cycle in all cases

Table 7: Calculated capacitance and specific capacitance for different graphite quantities

Graphite content (%)	Capacitance (mF)	Specific Capacitance (mF/g)
2	3	1.875
4	4	2.5
6	14	8.75
8	37	23.12
10	32	20

Figure 25 shows the variation of cell capacitance with graphite content. The curve rises slowly initially, followed by a sharp increase in capacitance between 6% graphite and 8% graphite content. No significant rise in capacitance was noticed beyond 8% graphite content.

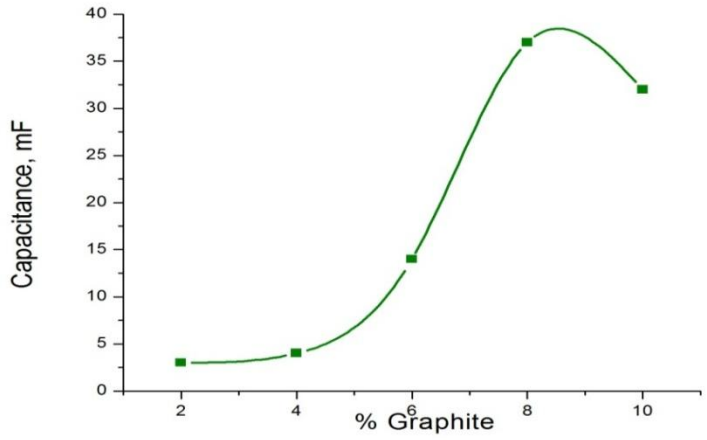

Figure 25: Variation of capacitance with graphite content (CV)

Figure 26 shows the cyclic voltammetry curves for ABS – graphite composites with varying graphite content. The electrochemical cell was swept between 0 and 1V at a scan rate of 5mV/s. The change in current with potential was recorded.

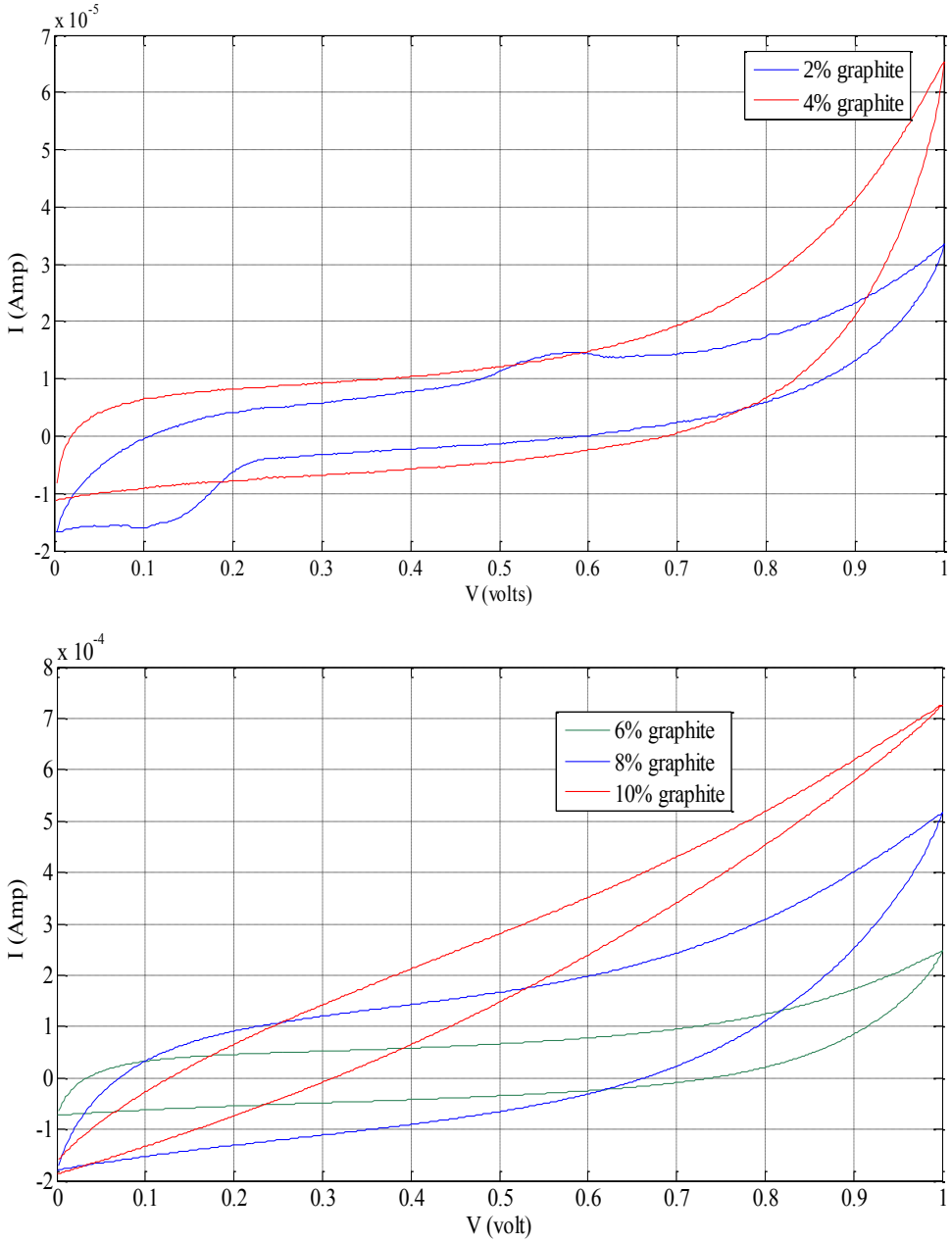

Figure 26(a) and 26(b): Cyclic Voltammetry curves for ABS – graphite (2, 4, 6, 8 and10%) composites

Both 6% and 8% graphite composites have CV curves that resemble a rectangular shape indicating charge storage through formation of a double layer. However 10% graphite does not have a rectangular shape.

From both Figure 23 and 25, one can see a sharp rise in capacitance between 6% and 8%. This sharp rise can be attributed to percolation behavior of ABS – graphite composites and this phenomena has been studied in detail by Balogun et al.[33].

3.2.4 Effect of pressing temperature on capacitance of ABS samples

ABS begins to flow at temperatures above 80^0C. The effect of heating temperature on the capacitance of ABS – graphite electrodes was analyzed. The electrodes were prepared from compositions varying between 2-10% and were pressed at 100^0C and 130^0C temperatures. Table 8 provides comparative capacitance data for ABS – graphite samples pressed at 100°C and 130°C. The cell capacitance was measured from both EIS and CV curves.

Table 8: Effect of pressing temperature on overall capacitance

ABS – Graphite Composition	**100^0C**		**130^0C**	
	EIS (mF)	**CV (mF)**	**EIS (mF)**	**CV (mF)**
2	3	3	2	2
4	6	4	4	4
6	20	14	13	7
8	65	37	23	12
10	69	32	27	17

From the above table we can see that the capacitance is higher in the case of 100^0C pressing temperature as compared to 130^0C. This change in capacitance is due to the low surface area of the electrode material that is exposed to the electrolyte. At 130^0C temperature, the polymer is able to flow more, completely forming a smooth surface with very low porosity. On the other hand electrodes pressed at 100^0C have higher porosity. The presence of pores allows the electrolyte to penetrate deeper into the sample and hence more area is available for double layer formation.

3.2.5 Dependence of capacitance on particle size of ABS

The particle size of ABS powder obtained from Sigma – Aldrich was <1100 μm. The powder was sieved into particles of different size range. ABS -8% graphite composites were made with these particles and were characterized using cyclic voltammetry tests. ABS – 8% graphite was chosen because it showed the best supercapacitor behavior among all the composites. Table 9 gives us the cell capacitance and capacitance as a function of area for three different ABS particle size range. The capacitance was evaluated from the CV plots obtained for the composites with 0.1M KOH electrolyte.

Table9: Capacitance data for different particle sizes

ABS Particle size	**Cell capacitance (mF)**	**Capacitance as function of area (mF/cm^2)**
<150 microns	17.90	1.768
150 – 500 microns	3.991	0.394
>500 microns	2.251	0.22

Figure 27 below shows the variation of capacitance with particle size. One can see that capacitance is much higher for ABS - graphite composite with smaller ABS particles compared to ABS – graphite composite with large ABS particles.

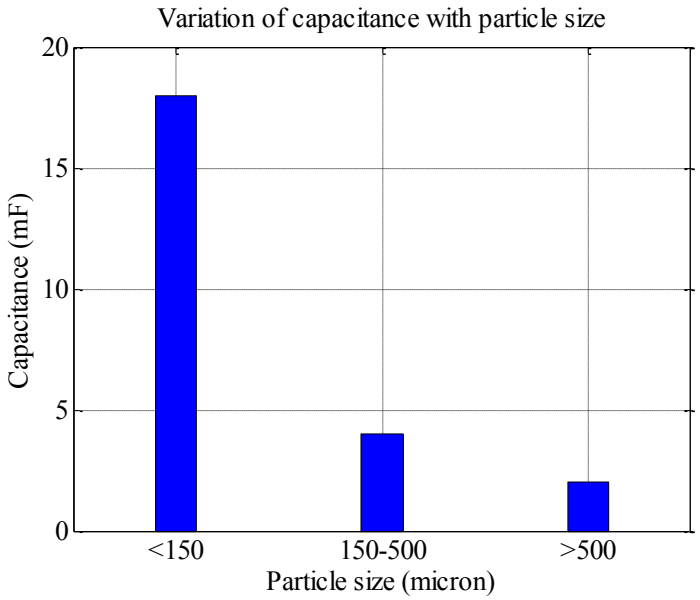

Figure 27: Capacitance with Particle size

This data can be explained by the fact that smaller the size of the particles, more region is available between the grains for graphite to be exposed to the electrolyte. With higher surface area, more active sites are available for the ions in the electrolyte to form a double layer. This results in larger amount of charge stored and higher capacitance.

The capacitance of ABS-graphite composites was found to be in mF range. The low capacitance is mainly due to the fact that the capacitance is purely double layer. The conductivity is important from a kinetic standpoint and though the conductivity rises sharply at the percolation threshold, the active sites for double layer formation are only between ABS grains, while the bulk ABS matrix does not play a significant role in double layer capacitance.

Chronopotentiometry tests showed that the charge loss is very high, which reduces the efficiency of supercapacitor.

3.2.6 SEM and optical microscope images of ABS-8% graphite samples

Figure 28 shows the SEM and optical microscope images for ABS – 8% graphite composite pressed at 100°C.

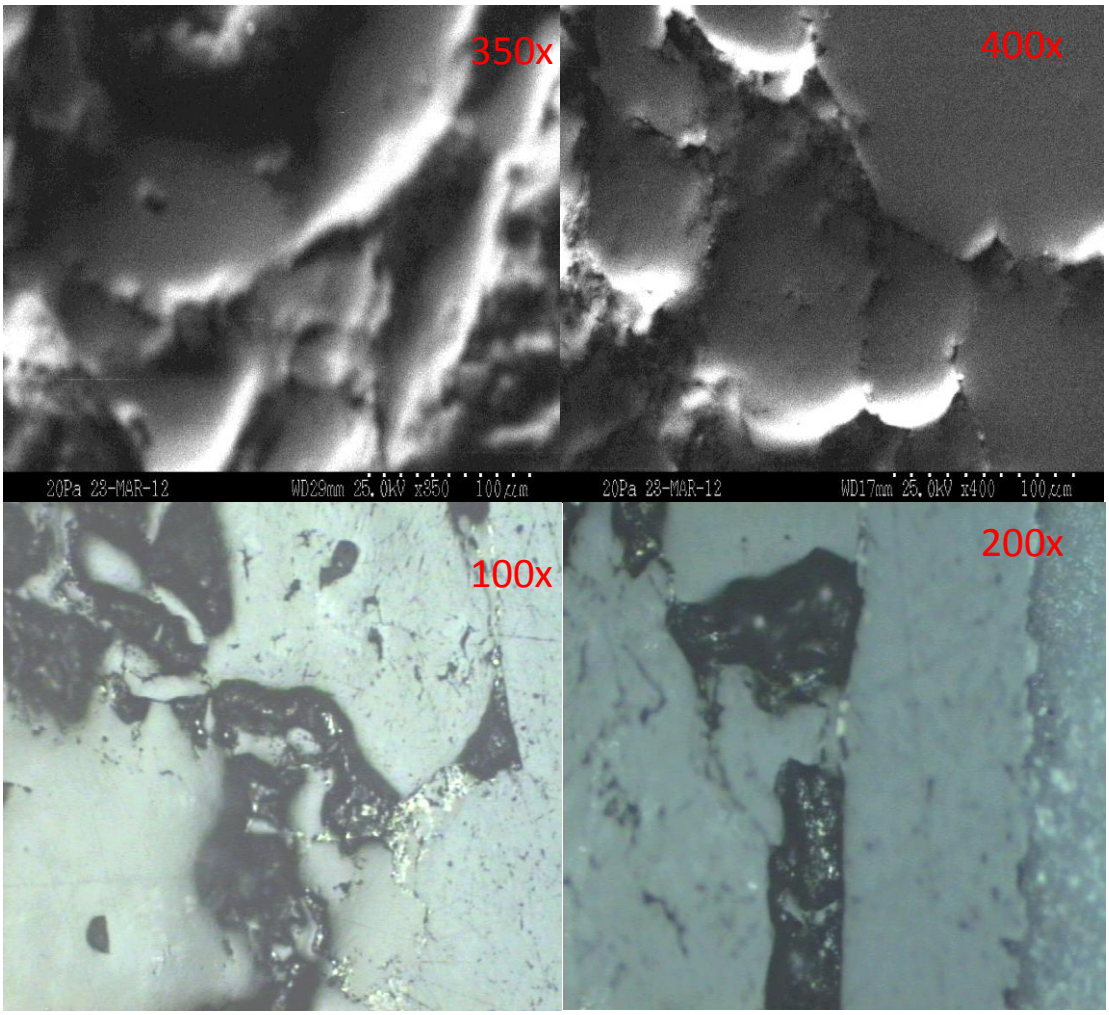

Figure 28: SEM and Optical microscope images of ABS – 8% graphite at 350x, 400x, 100x and 200x respectively

The SEM and optical microscope images show graphite deposited between ABS grains. ABS does not fuse completely as complete flow is not obtained at 100°C. This helps increase the graphite content exposed to the electrolyte.

3.3 Comparison between ABS and PANI

ABS is an inherently non – conducting polymer. PANI obtained from Sigma Aldrich had a conductivity of 2-4 S/m. The supercapacitor nature of composites with PANI and ABS as the bulk matrix was compared by preparing composites with 10% graphite. Both composites were pressed into pellets and were used as electrodes in the two electrode cell.

Table 10 below, gives a comparison between the capacitance of ABS based composites and PANI based composites. The capacitance for the PANI composite is a lot higher than that of ABS composite.

Table 10: Calculated capacitance values from ABS and PANI composites with graphite

Filler material: 10 % graphite	**EIS**		**CV**	
	Capacitance (mF)	**Specific Capacitance (mF/g)**	**Capacitance (mF)**	**Specific Capacitance (mF/g)**
ABS	69	43.12	32	20
PANI	236.45	147.78	95.92	59.95

The higher capacitance is due to the fact that both PANI and graphite contributes to the overall capacitance of the electrochemical cell. In the case of ABS composite, only graphite forms a

double layer. ABS provides mechanical strength to the composite. PANI on the other had has good conductivity and contributes to the overall capacitance. The polyaniline composite has higher porosity than ABS composite. This increases the overall surface area that is exposed to the electrolyte.

3.4 Comparison between graphite and activated carbon

Polyaniline composites were prepared using graphite (115 m^2/g) and activated carbon (900 m^2/g) as filler materials. The composites were pressed into pellets and characterized electrochemically using 0.1 M KOH as the electrolyte.

Figure 29 gives the EIS curves for both the electrodes. At higher frequencies, the EIS curve resembles a depressed semi-circle, which tells that the electrochemical behavior is kinetic controlled [31].

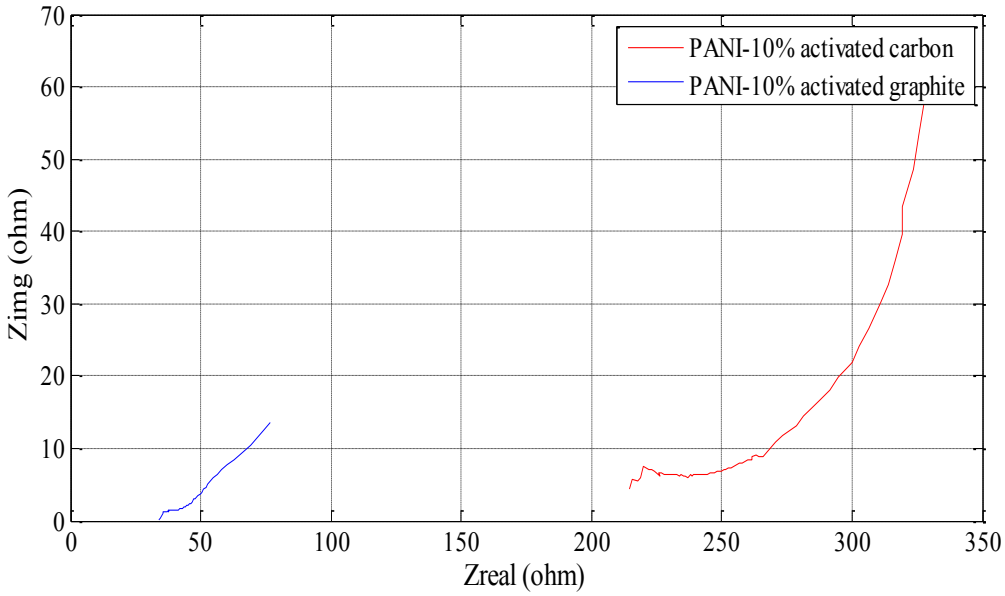

Figure 29: EIS curves for PANI composites with graphite and activated carbon

The fact that the Warburg region is more towards the vertical indicates that both electrodes have capacitor properties. The vertical nature is more prominent in the case of activated carbon as compared to graphite which has an approximately 45^0 incline.

Figure 30 shows the cyclic voltammetry curves of both the samples. The activated carbon curve has a higher area and peak current when compared to the graphite composite.

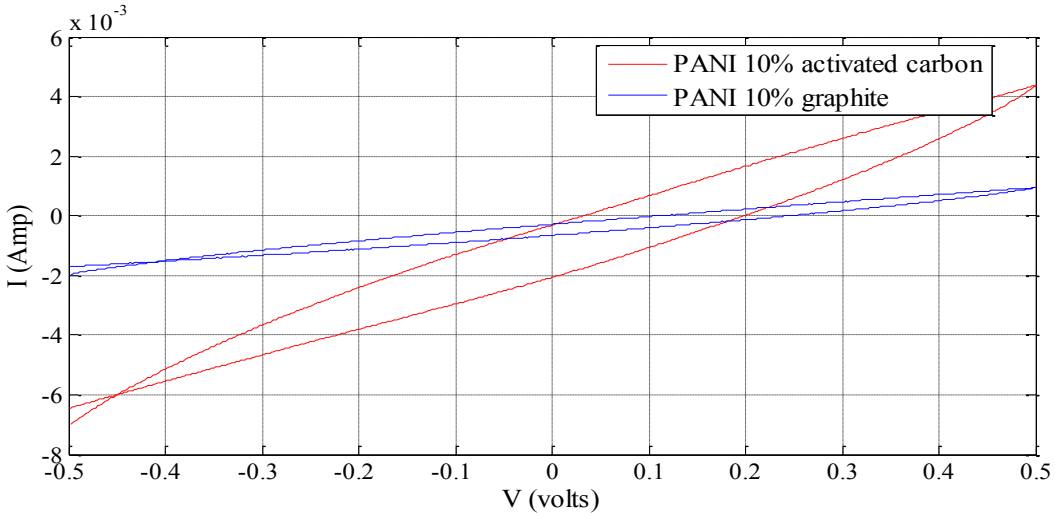

Figure 30: CV curves for PANI composites with graphite and activated carbon

Table 11 below gives the capacitance values for the two electrochemical cells calculated from the EIS and CV curves. The capacitance and specific capacitance for PANI – activated carbon composite based electrochemical cell is larger when compared to PANI – graphite composite electrodes.

Table11: Capacitance and specific capacitance for PANI based composites

Composite	EIS		CV	
	Capacitance (F)	**Specific capacitance (mF/g)**	**Capacitance (F)**	**Specific capacitance (mF/g)**
PANI – 10% graphite	0.23	147.78	0.09	59.95
PANI – 10% activated carbon	1.165	728	1.04	650

The PANI - activated carbon composite displayed much higher capacitance. The high surface area of the activated carbon results in more active sites available for the formation of a double layer. The overall cell capacitance for the PANI – activated carbon electrodes was in the range of 1F, which is very high and indicated the supercapcitor nature of the material. The specific capacitance is in mF/g range. The lack of redox peaks in the CV curve tells us that there is no redox capacitance contribution to the overall capacitance.

3.5 PANI – 10% activated carbon in a three electrode cell

All tests that performed previously are based on a two electrode setup developed in the laboratory. In the two electrode setup, the composite material tested played the role of the reference, working and counter electrodes. In the case of a three electrode setup, only the working electrode was composite material. Platinum plays the role of counter electrode and the reference electrode was the saturated calomel electrode. The three electrode setup gives us

insight of the capacitance properties of the material. The two electrode setup gives us more details about the electrochemical cell properties. In a two electrode setup, the cell capacitance and capacitance as a function of area were used as a basis of comparison. Specific capacitance has higher relevance in the case of a three electrode setup. All three electrode measurements were performed using a standard electrochemical flat cell.

The composite was coated onto a silver disc manually and the coating was then allowed to dry in an oven at the temperature of 40^0C for 10 minutes. The weight of the composite exposed to the electrolyte was 0.01 g. A filter paper separator was used to prevent any surface damage to the material. The electrolytes used were 0.1 M KOH and 1M H_2SO_4. The setup was allowed to stabilize for 30 minutes before electrochemical characterization.

The EIS curve for PANI – 10% activated carbon in a three electrode cell is shown in Figure 31. The test was performed at 0.75V between 10000Hz and 0.01Hz frequency.

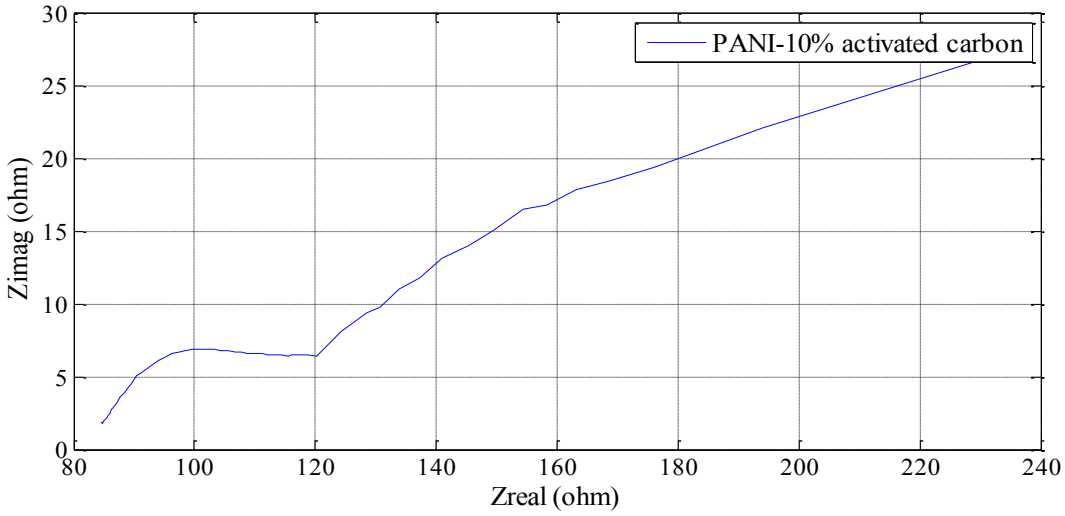

Figure 31: EIS curve for PANI – 10% activated carbon in a 3 electrode setup with 0.1 M KOH

A depressed semi-circle was observed at higher frequencies. At lower frequencies, there is a rise in the Warburg curve, which indicated the capacitor properties of the material.

Figure 32 below shows the cyclic voltammetry curve for the same electrochemical cell. The test was performed after EIS test. The scan rate used was 5 mV/s. The tests were performed between -0.2V and 0.8V. The curve shows the supercapacitor nature of the material. The center of the curve is rectangular and the peak at 0.26 V shows indicates PANI reduction. The peak current reached is around 3.5 mA, which is much higher than any previous electrode material tested. The capacitance calculated from EIS curve is 0.945 F and that from the CV curve is 508.31 mF. The specific capacitance in these cases corresponds to 94.5 F/g and 50.83 F/g. The capacitance is pseudo-capacitive in nature.

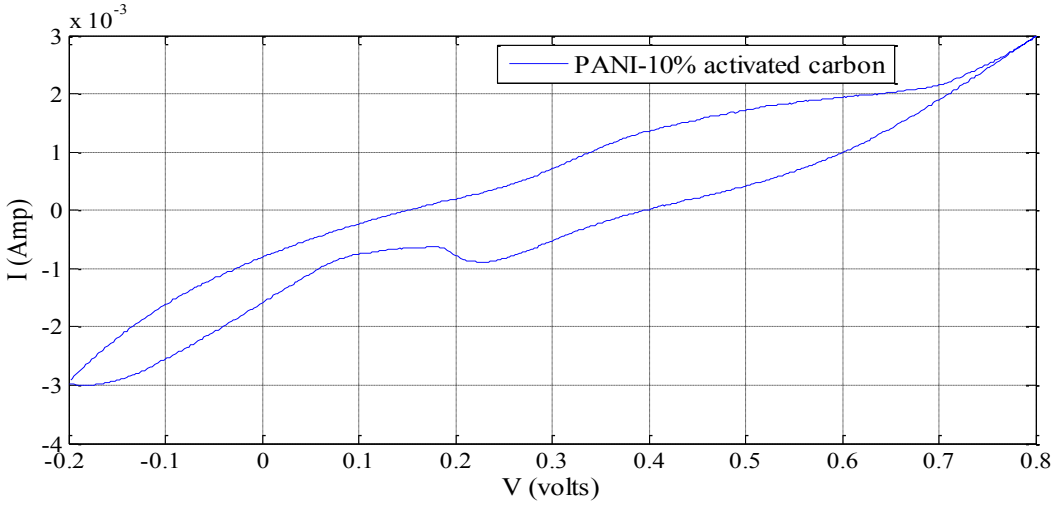

Figure 32: CV curve for PANI – 10% activated carbon in a 3 electrode setup with 0.1 M KOH

0.1 M KOH is a base electrolyte. The composite was tested with 1M H_2SO_4 which is a strong acidic electrolyte. Figure 33 shows the EIS curve for PANI – 10% activated carbon electrodes in a three electrode cell with 1M H_2SO_4 electrolyte. The overall impedance of the electrochemical

cell was found to be lesser compared to 0.1 M KOH electrolyte. The electrochemical cell showed low bulk resistance and charge transfer resistance.

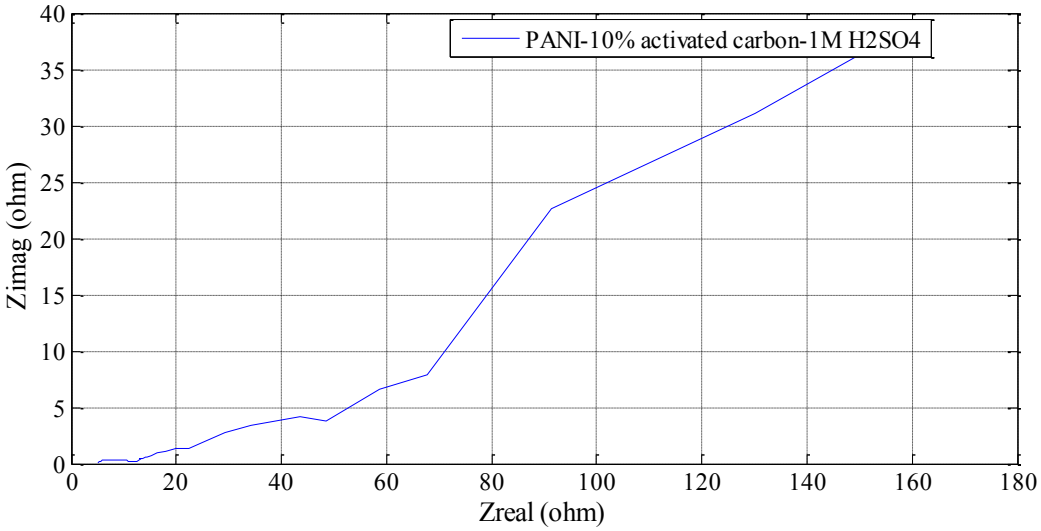

Figure 33: EIS curves for PANI – 10 % activated carbon with 1M H2SO4 electrolyte

Figure 34 shows the CV curves for the same cell. The electrochemical cell was swept between -0.2V and 0.8V. The curve has a broad region between -0.2V and 0.4 V with redox peaks at 0.3 V and 0.65V.

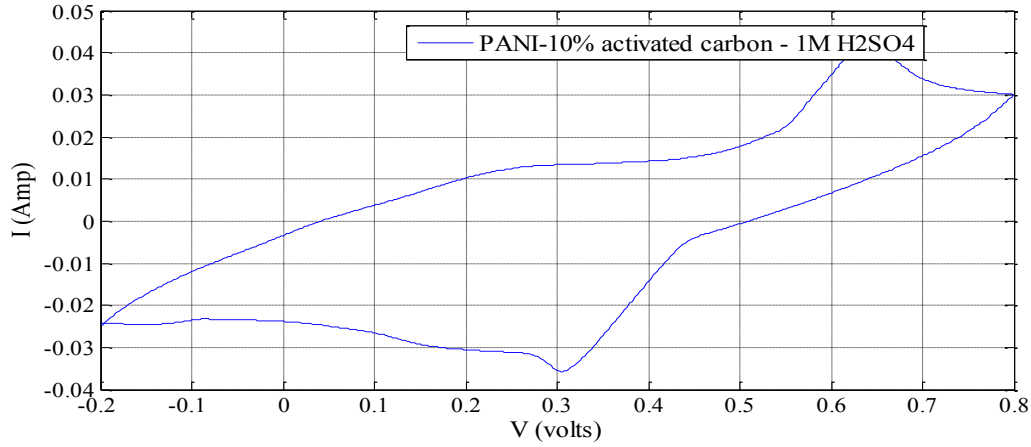

Figure 34: CV curves for PANI – 10 % activated carbon with 1M H2SO4 electrolyte

The peak currents reached in this case are as high as 45 mA and the curve showed excellent supercapacitor properties. Apart from the large rectangular portion, oxidation and reduction peaks for PANI was seen at 0.3V and 0.65V. The peaks correspond to transformation of PANI from emaraldine state to leucoemaraldine and pernigraniline states. [34,35].

3.6 Comparison between two electrode and three electrode cell

A two electrode cell with the same electrode (paste of PANI - 10% activated carbon) and 1M H_2SO_4 electrolyte was compared to the data obtained from a three electrode cell. The electrodes were coated onto silver discs. Figure 35 shows the EIS curve for the electrochemical cell. A depressed semi – circle was seen between 2 ohms and 6 ohms following which the curve rose vertically.

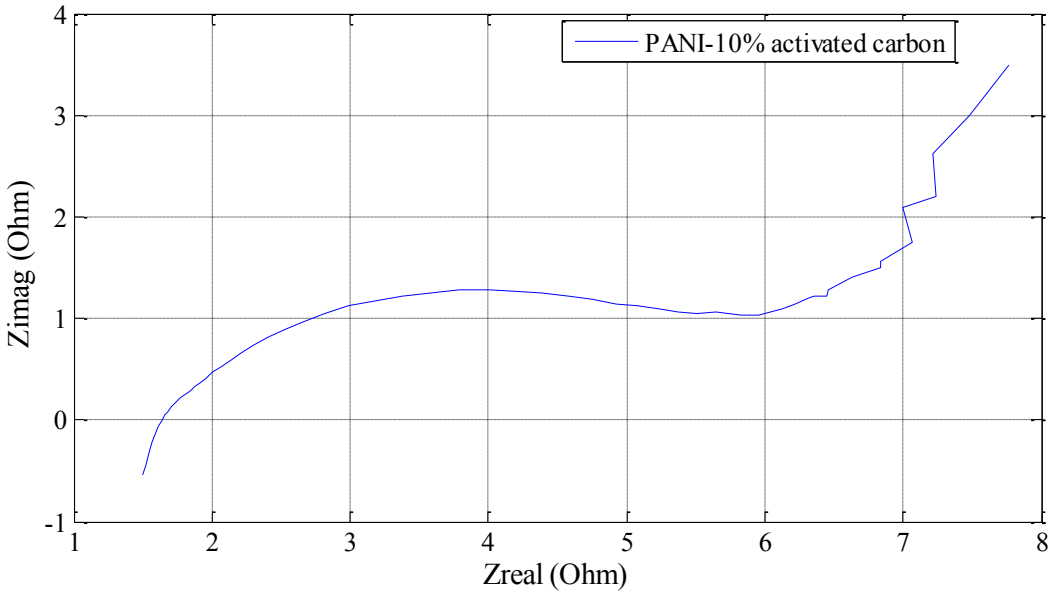

Figure 35: EIS curve for PANI – 10% activated carbon in a two electrode setup

The overall impedance of the two electrode cell was lower than that of the three electrode cell. The Warburg curve had a near vertical incline. A vertical Warburg curve is commonly seen in electrodes with good supercapacitor properties.

Figure 36 shows CV curves for the polyaniline-10% activated carbon samples in a two electrode system. The cyclic voltammetry curve for the cell showed good supercapacitor behavior. The region between -0.2V to 0.4 V is largely rectangular. Above 0.4V, the contribution to the overall capacitance is less. Pairs of redox peaks are seen at -0.2V, -0.5V, 0.2V and 0.4V. These peaks represent the reversible transformation of the composite from emaraldine state to leucoemaraldine and perigraniline states. Also at 0.4 V, the cell reaches a steady state current rapidly and the overall charge-discharge performance is reversible between -0.2V and 0.4V. Hence the electrochemical cell displayed excellent capacitance properties in this region.

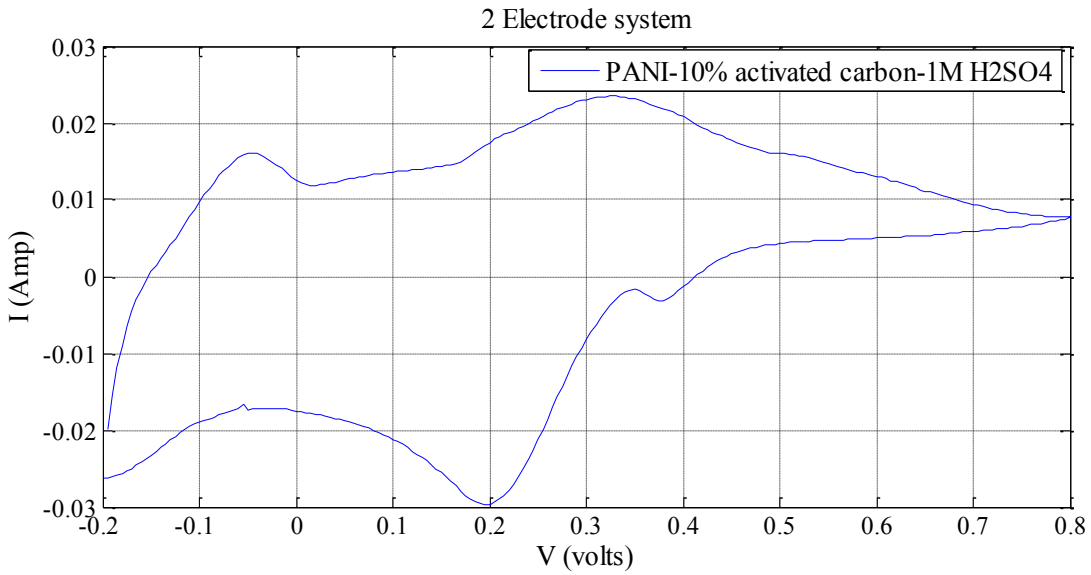

Figure 36: CV curve for PANI – 10% activated carbon in a two electrode setup

Table 12 below gives the capacitance and specific capacitance calculated from the above two figures. One sees that the actual material capacitance was much higher than the cell capacitance.

The physical milling method used to prepare the composite is easy and also ensured that the carbon dispersed uniformly in the composite.

Table 12: Capacitance and specific capacitance for two electrode and three electrode setup

Cell	EIS		CV	
	Capacitance (F)	**Specific Capacitance (F/g)**	**Capacitance (F)**	**Specific Capacitance (F/g)**
3 electrode cell	0.404	40.45	7.261	726.1
2 electrode cell	0.454	4.540	5.387	53.87

Specific capacitance of 726.1 F/g and 53.87 F/g were observed for PANI – 10% activated carbon composites. From these data one can say that the PANI – 10% activated carbon composite with 1M H_2SO_4 performed best among all the measurements in this work. The electrode material was also stable after the electrochemical tests. Further analysis of the charge-discharge characteristics of the electrode material was performed using chronopotentiometry tests.

3.7 SEM images of PANI – 10% activated carbon electrodes

Figure 37 shows the PANI electrode surface. The images were taken before the composite was used in an electrochemical cell. The electrodes show high porosity which is good for electrolyte penetration.

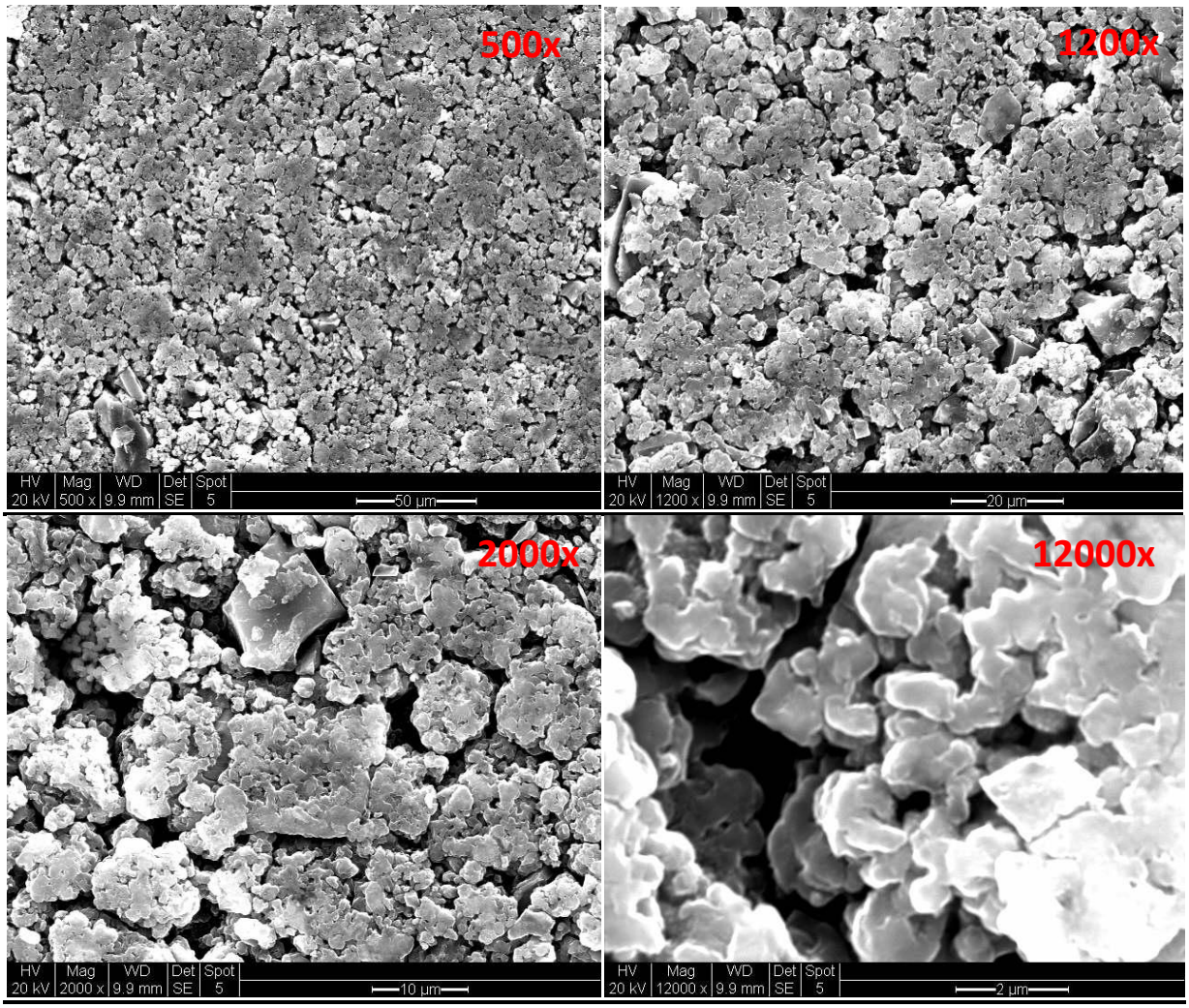

Figure 37: SEM images of PANI – 10% activated carbon samples at 500x, 1200x, 2000x and 12000x magnifications

3.8 Chronopotentiometry studies of PANI – 10% activated carbon composite

The charge-discharge characteristics of PANI – 10% activated carbon composite were evaluated using chronopotentiometry. These tests were performed for both two electrode and three electrode electrochemical cells with thin coating of the composite with 1M H_2SO_4 as the electrolyte. Figure 38 gives the increase/ decrease in voltage with time. The cell was charged to peak voltage of 0.45 V at 4 mA in 200 seconds and then discharged for 75 seconds.

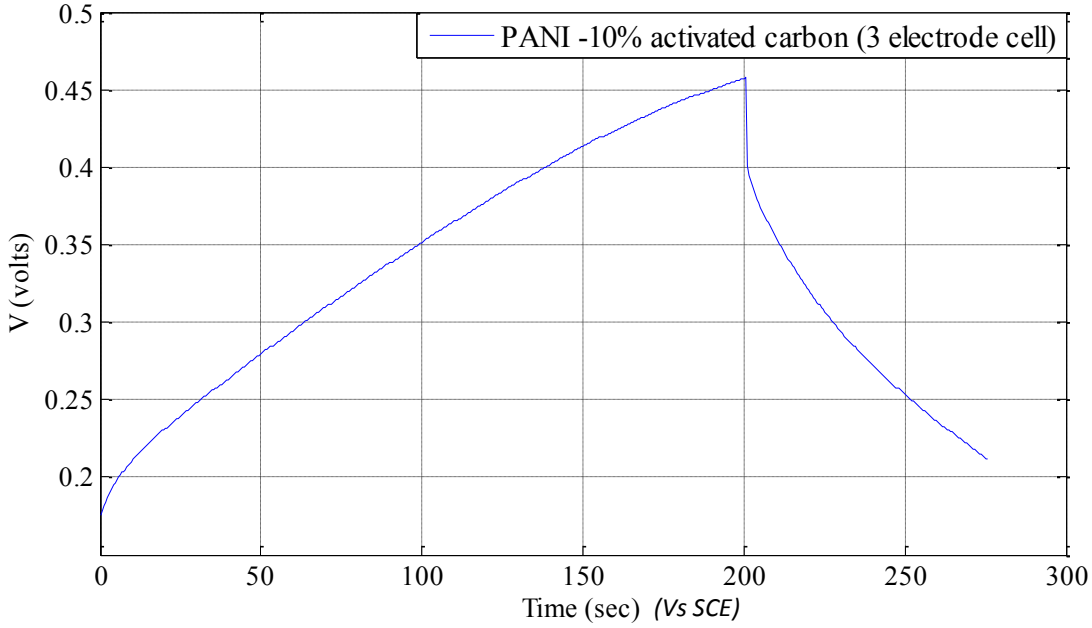

Figure 38: Chronopotentiometry curve for PANI – 10% carbon composite in a three electrode setup at 6mA current

The triangular nature of the charge-discharge curve shows the supercapacitor nature of the electrochemical cell. The initial *iR (voltage drop due to internal resistance)* drop during discharge is small which means that there is very low internal resistance. Table 13 below shows

the capacitance, energy and power density calculated from the above curve. The capacitance, energy and power densities were calculated for the discharge cycle.

Table 13: The power and energy density values obtained from the chronopotentiometry scan at 4 mA

Composite	Capacitance (F)	Specific Capacitance (F/g)	Energy Density (Wh/kg)	Power Density (W/kg)
PANI -10% activated Carbon	1.6	160	1.76	84.82

From the above table one can see that the cell has high specific discharge capacitance of 160 F/g. The power density of the cell was also high, but the low energy density may limit its applications.

The chronopotentiometry scan was also performed for the same composite in a two electrode setup under the same conditions to determine the performance of an actual capacitor. Figure 39 and 40 below shows the voltage versus current profile at 4mA and 6 mA charge/ discharge current respectively. The cells were charged for 200 seconds and were then discharged for 75 seconds. Peak voltage values reached were 0.145V and 0.198V respectively.

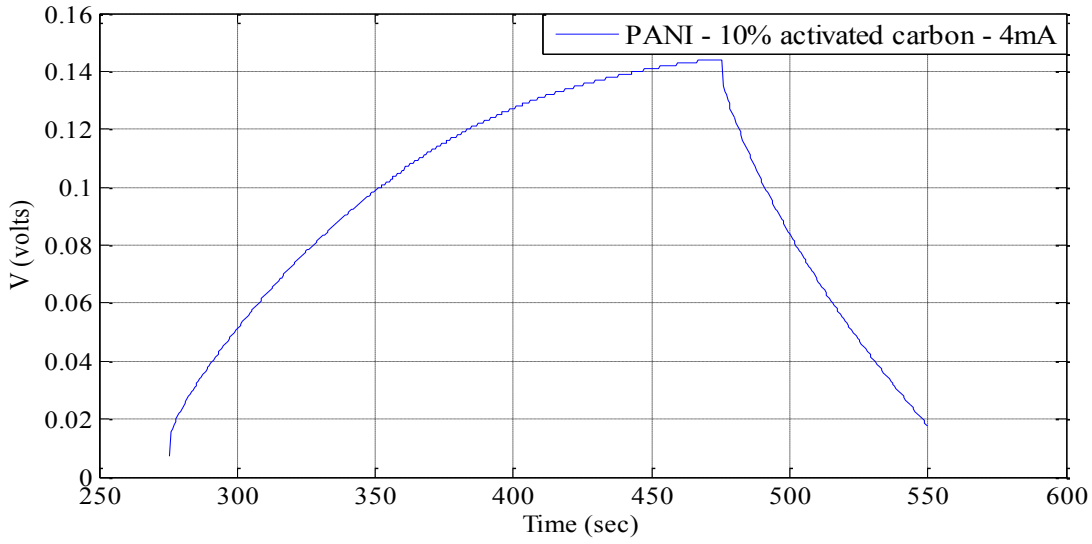

Figure 39: Chronopotentiometry scan at 4 mA

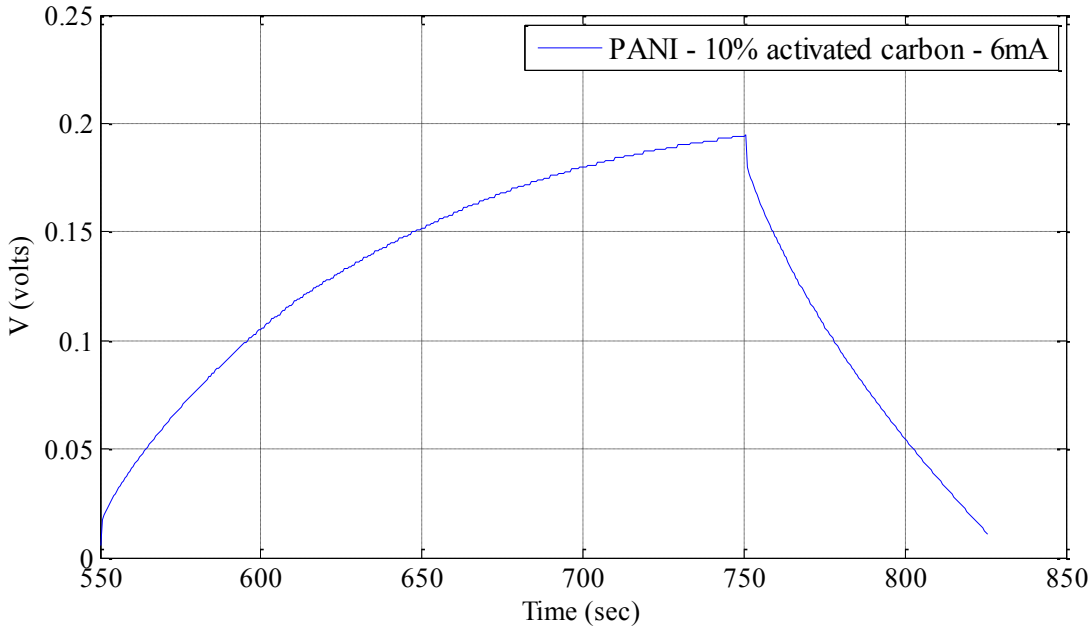

Figure 40: Chronopotentiometry scan at 6mA

Since both the electrodes are the same, the complete discharge state is 0V. From the above figures, one can see that the charge – discharge curve resembled that of a supercapacitor. The *iR*

drop is very low in both cases.. Table 14 below gives the specific capacitance of the cell calculated from the charge-discharge behavior. Capacitance is also expressed as a function of electrode area.

Table 14: The cell capacitance of the composite in the two electrode setup at 4 mA and 6 mA

Current(mA)	Capacitance (F)	Specific Capacitance (F/g)	Capacitance as function of area (F/cm^2)
4	2.36	23.0	0.233
6	2.45	24.5	0.242

3.9 XRD analysis of PANI – 10% activated carbon composite

Figure 41 shows the XRD analysis of PANI – 10% activated carbon. The peaks at around 20.8^0 and 25.0^0 are for (020) and (200) planes of PANI as an emaraldine salt [36, 37].The (002) and (102) planes for carbon corresponds to hexagonal graphite structure which shows that the carbon has high electrical conductivity [36].

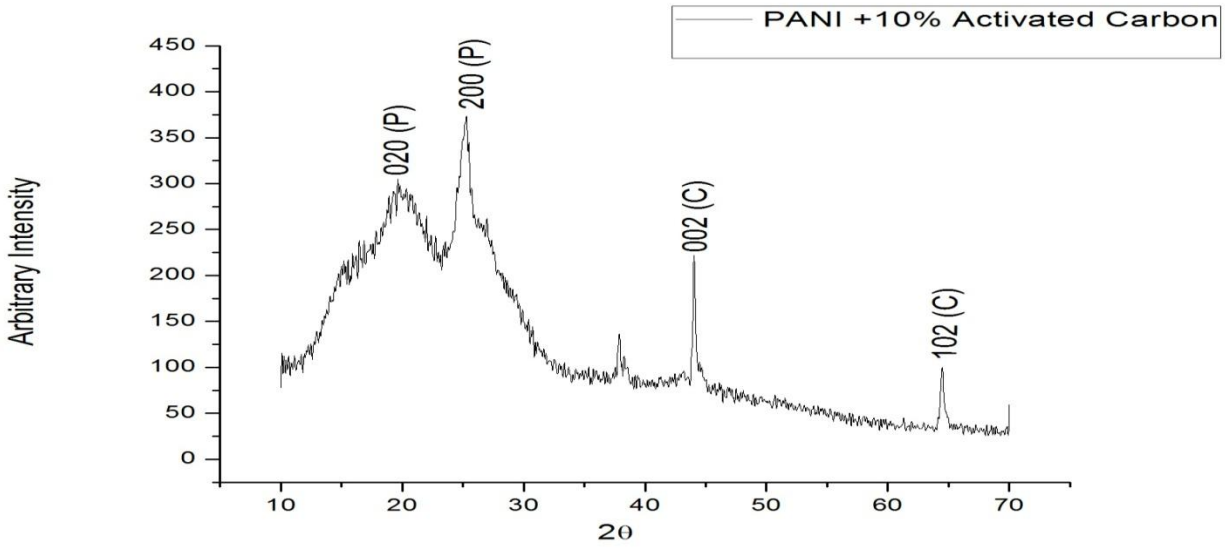

Figure 41: XRD of PANI – 10% activated carbon composite

3.10 Copper ferrocyanide as electrode material

In the previous studies, we had evaluated and compared the capcitive nature of polymer-carbon based composites. The copper ferrocyanide used as electrodes were developed in the lab. The powder was coated on a silver disc and was characterized using 0.1 M KOH electrolytes in the two electrode setup.

Figure 42 below shows the cyclic voltammetry curve for copper ferrocyanide. The curve has a rectangular shape with peaks at -0.037 V and 0.11V. The overall capacitance of the cell is 5.8 F. The nature of the curve shows us that the rectangular region is very small and greater contribution to cell capacitance is from the redox reactions.

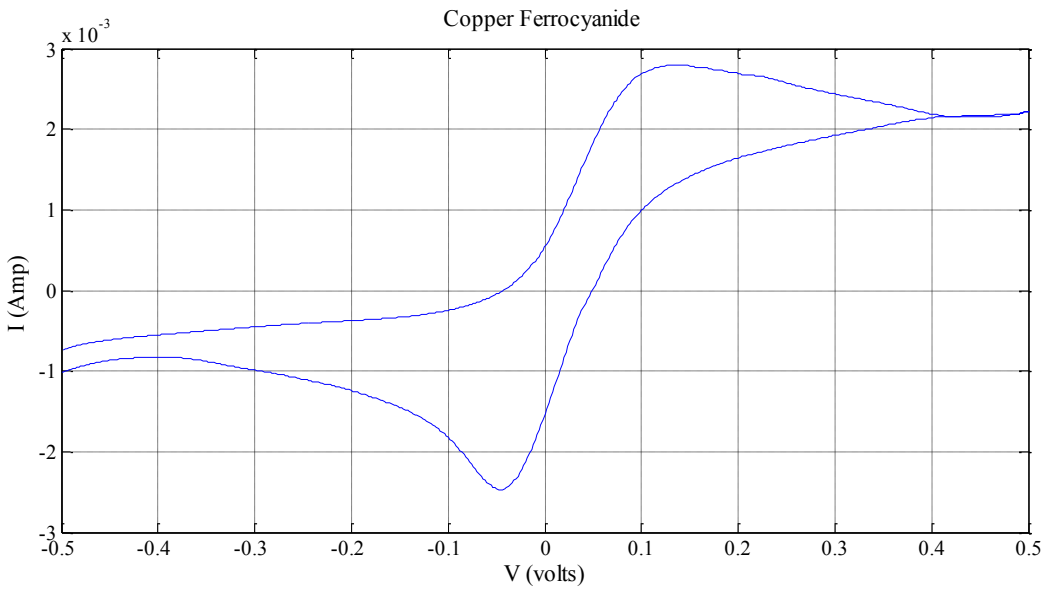

Figure 42: CV curve for Copper Ferrocyanide electrodes

Figure 43 shows the SEM images for copper ferrocyanide material. The images were taken at 800x and 3500x magnifications.

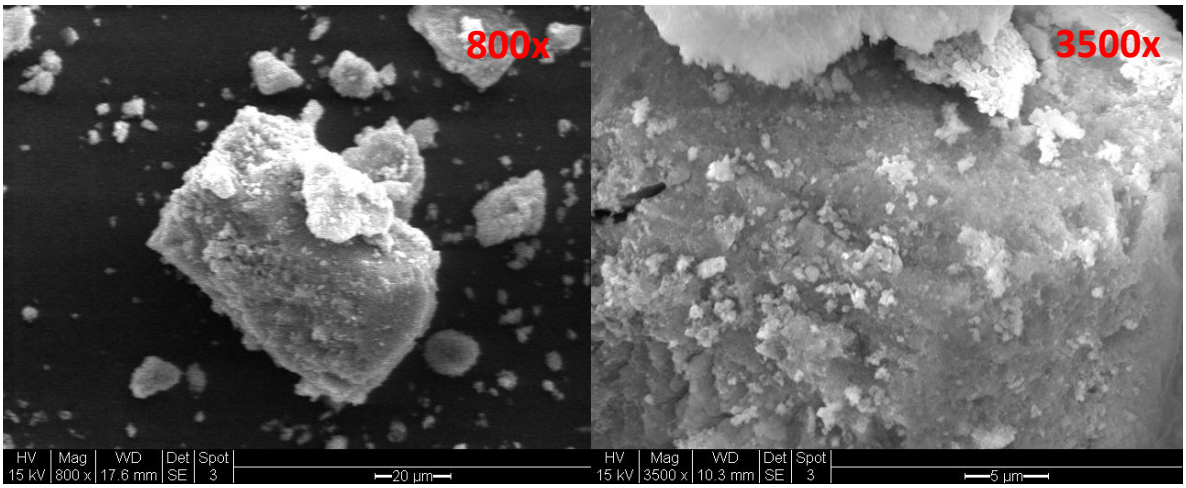

Figure 43: SEM images of copper ferrocyanide powder at 800x and 3500x magnifications

Figure 44 below shows the EDX elemental mapping analysis of copper ferrocyanide samples. Potassium from potassium permanganate was present in the sample in small amounts and acts as an impurity. Potassium showed up in the EDX mapping analysis.

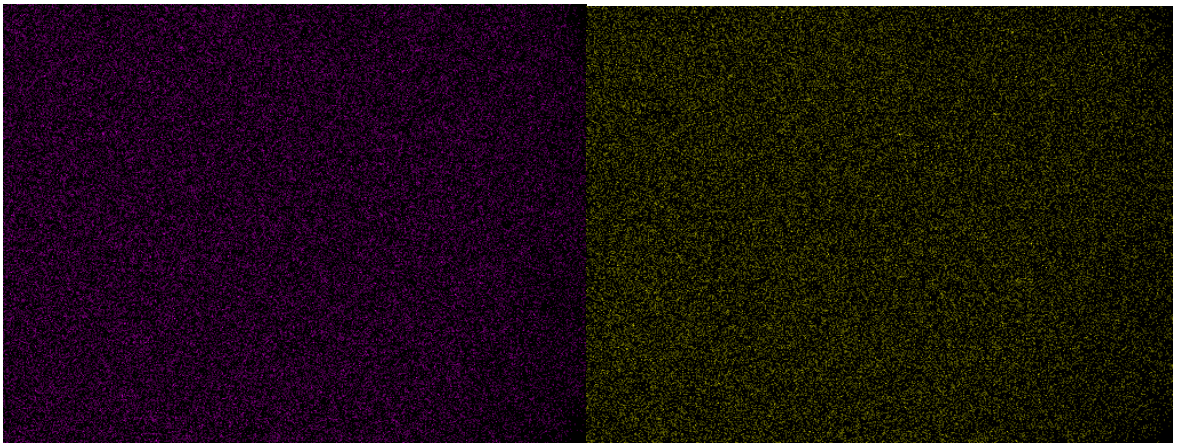

Copper Iron

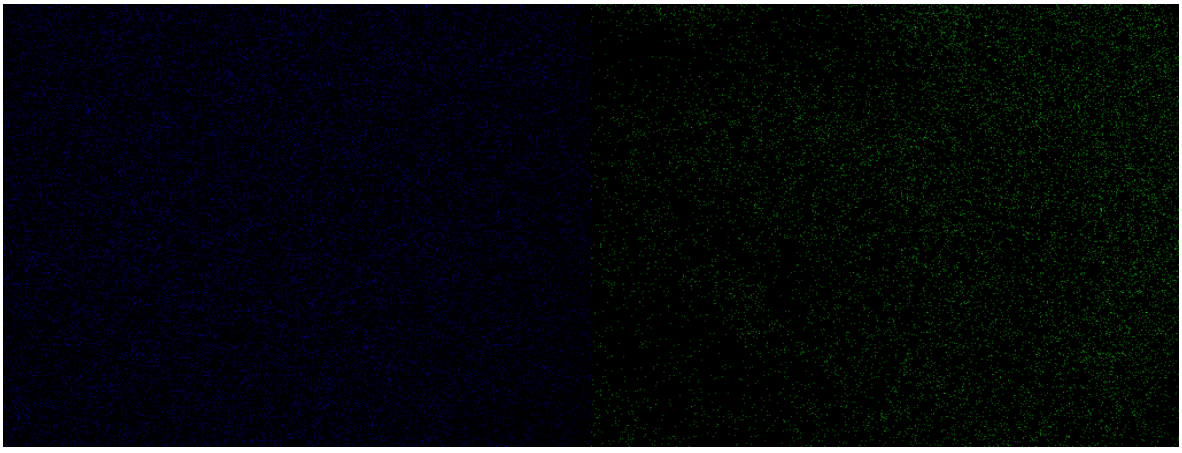

Potassium Nitrogen

Figure44: EDX mapping analysis of copper ferrocyanide electrodes

3.11 XRD analysis of copper ferrocyanide

Figure 45 shows the x-ray diffraction analysis of copper ferrocyanide samples. The x-ray diffraction analysis confirmed the presence of copper ferrocyanide compound with different phases. Upon evaluation, the sample was found to be highly crystalline (92.5%).

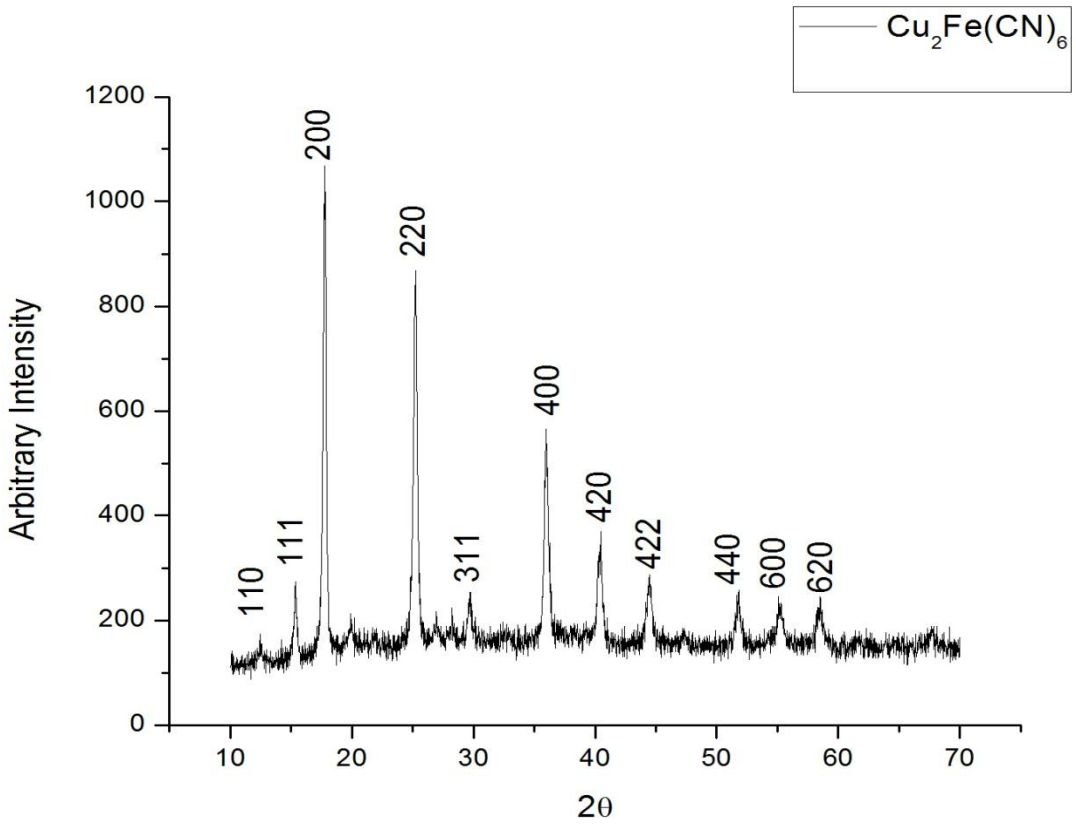

Figure 45: XRD analysis of copper ferrocyanide sample

3.12 Comparison between filter paper and cloth material as separator

The role of separator was analyzed by comparing filter paper with an absorbent fibrous cloth material as separators in a two electrode electrochemical cell with ABS – 6% graphite composite as electrodes. The filter paper was comparatively thinner than the cloth material and also had better wettability. On the other hand the cloth material was sturdier than filter paper. The electrolyte used in the comparison is 0.1 M KOH. The thickness of filter paper was 0.0079 inch and the thickness of cloth material was 0.0126 inch.

Figure 46 shows the EIS behavior of the two electrochemical cells. The test was performed at 0.75V between 300,000 Hz and 0.001 Hz. Both the separators have a very similar bulk resistance, charge transfer resistance and overall capacitance.

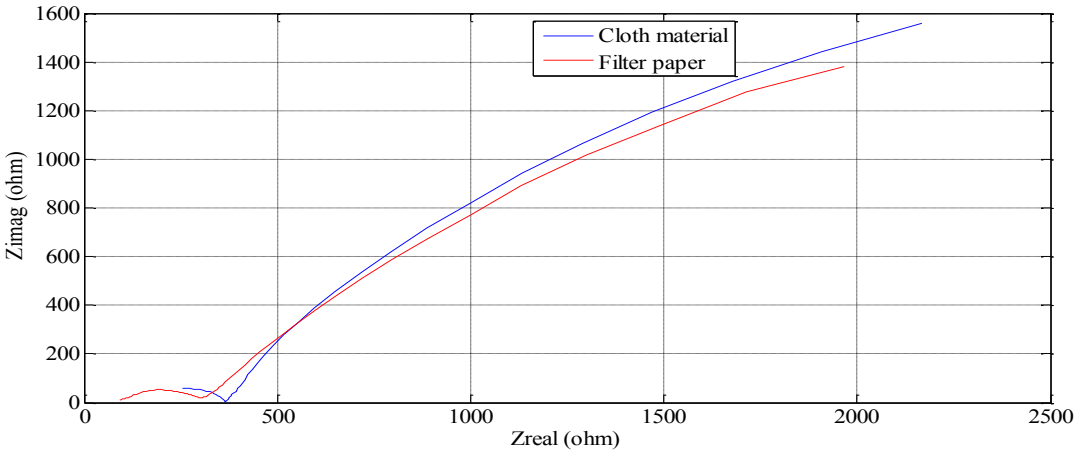

Figure 46: EIS curve for both separators

Figure 47 shows the CV curves for ABS – 6% graphite composite with filter paper and absorbent cloth material separators. The potential was scanned between 0 and 1V. The CV curves for the two cells resembled each other. In both cases, the cell displayed double layer capacitor behavior.

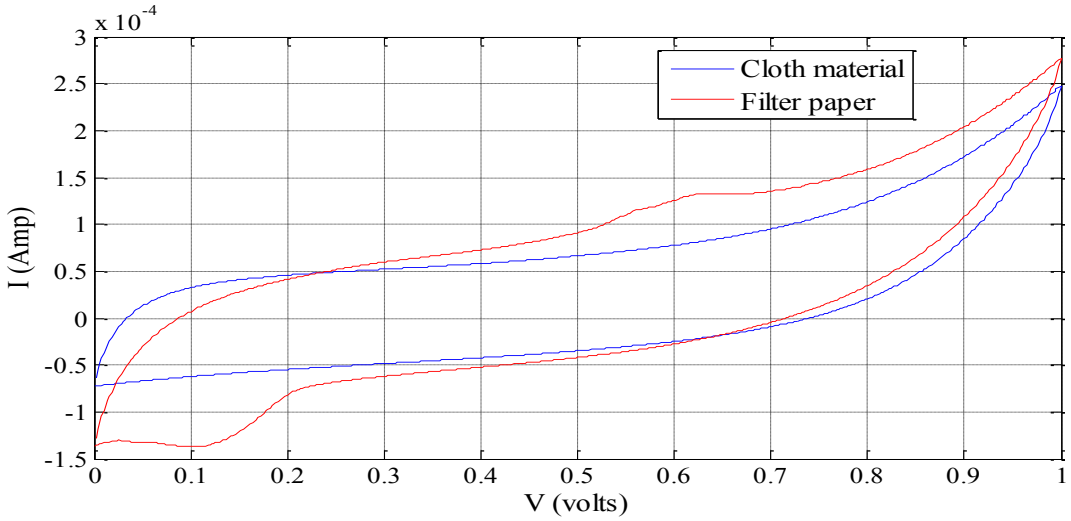

Figure 47: CV curve for both separators

The two separators compared had very different physical properties. Both electrochemical cells behaved very similarly. The separator material has to be optimized based on the electrochemical cell assembly.

3.13 Variation of capacitance with distance of separation

In the case of dielectric capacitors, the capacitance varied inversely with the distance of separation. But in electrochemical cells, the charge storage mechanism is completely different. In order to study the effect of distance of separation, experiments were performed with varying separator thickness (number of filter papers was increased). Thickness of one filter paper separator was 0.0079 inch. The measurements were made with PANI -15% activated carbon samples with 0.1 M KOH electrolyte.

Figure 48 shows us the change in cell capacitance with increase in distance of separation. There is a sharp decrease in with increasing thickness of the filter papers. This can be attributed to the increase in cell resistance due to the increase in separation. It is clear that high capacitance can

be achieved when the distance between the two electrodes is small. The electrodes should be as close to each other as possible without coming in contact.

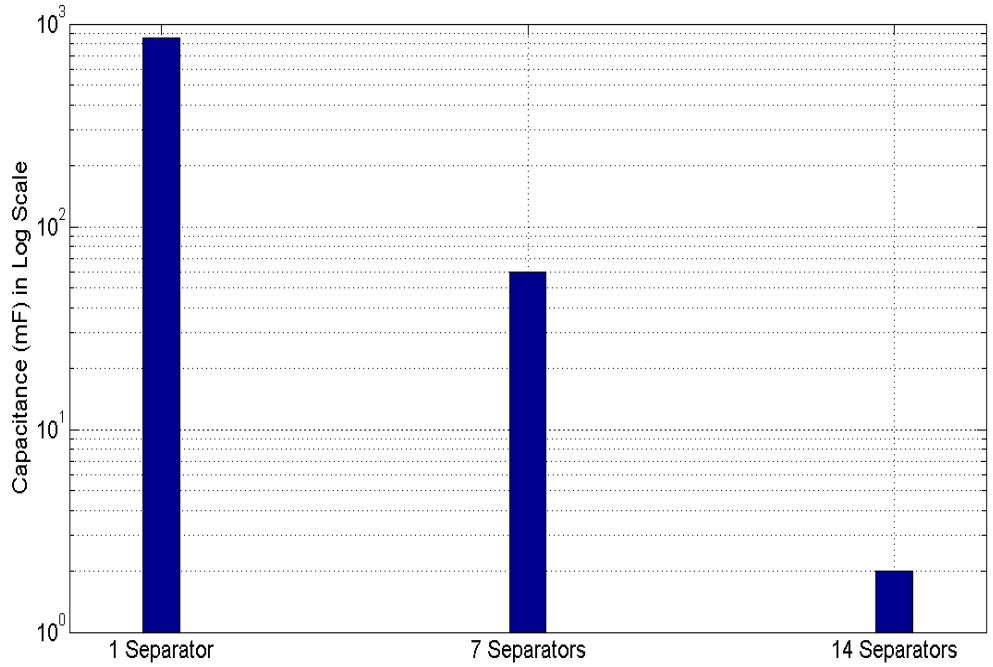

Figure 48: Variation of cell capacitance with separator thickness

SUMMARY

1. A two electrode electrochemical cell was successfully developed and calibrated. This cell was used to test the supercapacitor properties of ABS and PANI based conductive polymer composites. The performance of the cell was later compared to a standard three electrode cell. The two electrode cell was also used to compare electrochemical cell properties such as distance of separation and effect of separator on overall capacitance.
2. The capacitive behavior or ABS – graphite composites was studied in a two electrode cell setup. A sharp rise in capacitance was observed for ABS – graphite composites at the percolation threshold (6-8% graphite). The cyclic voltammetry curves displayed rectangular behavior indicating charge storage through double layer formation. The overall cell capacitance was in millifarad range. This was attributed to the fact that capacitance is purely double layer and the low number of active sites available for the formation of double layer.
3. Pressing the composite at a lower temperature increased the porosity of the electrodes thus improving electrode penetration. This in turn increased the overall capacitance as more graphite was exposed to the electrolyte for double layer formation. Use of smaller ABS particles also helped improve the capacitance. The larger region between ABS grains resulted in more graphite available on the surface.
4. PANI – graphite composite performed better than ABS – graphite composite. This was mainly due to role played by PANI in the overall capacitance of the cell. Apart from graphite, PANI also has active sites for double layer formation.
5. PANI – activated carbon had even higher capacitance value. The greater surface area of carbon resulted in more sites for double layer formation. The higher porosity of PANI

composites when compared to ABS composites also helped in achieving higher capacitance. The capacitance in the case of 1M H_2SO_4 electrolyte was pseudo-capacitance, as recognized from the presence of redox peaks in the cyclic voltammetry curves.

6. The performance of the two electrode cell was compared with that of a three electrode cell with 1M H_2SO_4 electrolyte. The three electrode cell gave us an understanding of the properties of the electrode material, while the actual cell capacitance was obtained from the two electrode cell. PANI – 10% activated carbon showed high specific capacitance and cell capacitance of 726 F/g and 5.387 F.
7. The charge – discharge nature of PANI- 10% activated carbon based electrochemical cell with 1M $H_2SO_4$was analyzed using chronopotentiometry. High discharge capacitance values were obtained showing the composite had excellent potential as a supercapacitor. The low energy density and good power density of the material limits it use to high power applications. The two electrode cell also showed very good discharge characteristics with high capacitance.
8. The role of a separator in an electrochemical cell was studied using filter paper and an absorbent fibrous cloth material. The EIS and CV curves for both separators were similar. The fibrous cloth material was sturdier than filter paper.
9. The effect of distance of separation on capacitance was studied by increasing the separator thickness. The capacitance dropped with increase in distance of separation. This is due to the increase in internal resistance. The electrodes must be as close to each other as possible while preventing contact.

CONCLUSIONS

1. A novel two electrode cell setup was developed in laboratory to investigate the electrochemical properties of conductive polymer composite electrodes and other cell properties.
2. The capacitance of ABS – graphite composites was nearly doubled between 6% and 8% graphite content. This rise could be due to the percolation threshold of the ABS – graphite system.
3. The capacitance of the ABS-graphite system was optimized based on ABS particle size and composite pressing temperature.
4. Composites with different charge storage mechanisms (ABS – graphite, PANI – graphite/ activated carbon) was compared and higher charge storage was achieved with pseudo-capacitance.
5. PANI – activated carbon composites showed high energy storage properties with 1M H_2SO_4 electrolyte. This composite was successfully incorporated in a two electrode cell setup. The electrochemical cell showed good supercapacitor characteristics between -0.2V and 0.4V.
6. The applicability of copper ferrocyanide as an electrode material in supercapacitors was investigated. The material showed good charge storage properties.
7. The role of separator and distance of separation between electrodes was studied. Reducing separation distance between electrodes improved charge storage.

FUTURE WORK

1. The application of ABS – graphite composites in supercapacitors, depends largely on improving its energy density. Further work is being performed to improve the conductivity of ABS – graphite composites by introducing other conducting materials
2. PANI – activated carbon composite displayed excellent supercapacitor properties but cell voltage was limited due to use of aqueous electrolytes. Further work is required to investigate the use of organic electrolytes (non – aqueous) and solid state electrolytes to improve energy density.
3. The cyclic stability of PANI – activated carbon composites over large number of cycles has to be evaluated.
4. Copper ferrocyanide shows promise as an electrode material for supercpacitors. Further work is however needed to understand its charge –discharge characteristics and cycle life.

REFERENCES

1. John Petersen; "Why America Must Focus On Domestic Energy Solutions Instead of Imports";
2. Shahriar Shafiee, Erkan Topal; "When will fossil fuel reserves be diminished?"; **Energy Policy,(37) 181–189 (2009)**
3. R. Ba˜nos, F. Manzano-Agugliaro, F.G. Montoya, C. Gil, A. Alcayde, J. Gomez; "Optimization methods applied to renewable and sustainable energy: A review"; **Renewable and Sustainable Energy Reviews ,(15) 1753–1766 (2011)**
4. Chuang Peng, Shengwen Zhang, Daniel Jewell, George Z. Chen; "Carbon nanotube and conducting polymer composites for supercapacitors"; **Progress in Natural Science ,(18) 777–788 (2008)**
5. Leyden jar. Encyclopedia Britannica Online. http://www.britannica.com/ed/ article-9048045 [2008-02-29].
6. Becker HI. US Patent 2 800 616, Low Voltage Electrolytic Capacitor. 1957.
7. Thomas Christen, Martin W Carlen; "Theory of Ragone plots"; **Journal of Power Sources, (91) 210-216 (2000)**
8. John R Miller, Patrice Simon; "Fundamentals of electrochemical capacitors design and operation"; **The Electrochemical Society interface, Spring 2008**
9. Yu Gao, Volker Presser, Lifeng Zhang, Jun J. Niu, John K. McDonough, Carlos R. Pérez, Haibo Lin, Hao Fong, Yury Gogotsi; "High power supercapacitor electrodes based on flexible TiC-CDC nano-felts"; **Journal of Power Sources, (201) 368–375 (2012)**
10. Adrian Schneuwly, Roland Galla; "Properties and applications of supercapacitors From the state of the art to future trends"; **Proceeding PCIM 2000**

11. Pankaj Arora and Zhengming (John) Zhang; “Battery Separators”; **Chem. Rev. (104) 4419-4462 (2004)**
12. F. Scholz (Ed.); “Electrochemical Methods – Guide to Experiments and Applications”
13. Chijuan Hu; “Fluid coke derived activated carbon as electrode material for electrochemical double layer capacitor”; Master of Applied Science thesis, Univeristy of Toronto
14. http://web.nmsu.edu/~snsm/classes/chem435/Lab14/double_layer.html
15. Pawan Sharma. T.S Bhatti; “A review on electrochemical double-layer capacitors”; **Energy conversion and Management, (51) 2901-2912 (2010)**
16. Tom Zawodzinski, Shelly Minteer, Gessie Brisard; “Physical and analytical electrochemistry: The fundamental core of electrochemistry”; **The Electrochemical Society Interface, Spring 2006**
17. Wei Chih-Chen, Ten-Chin Wen, Hsisheng Teng;”Polyaniline deposited porous carbon electrode for supercapacitor”; **Electrochemica Acta, (48) 641-649 (2003)**
18. WANG Qin, LI Jian-ling, GAO Fei, LI Wen-sheng WU Ke-zhong, WANG Xin-dong; “Activated carbon coated with polyaniline as an electrode material supercapacitors”; **New Carbon Materials, 23(3) 275–280 (2008)**
19. Chien-Ming Lai, Jing-Chie Lin, Kan-Lin Hsueh, Chiou-Ping Hwang, Keh-Chyun Tsay, Li-Duan Tsai, Yu-Min Peng; “On the electrochemical impedance spectroscopy of direct methanol fuel cell”; **International Journal of Hydrogen Energy, (32) 4381 – 4388 (2007)**

20. S.V. de Lima, H.P. de Oliveira; "Melting point of ionic ternary systems (surfactant/salt/water) probed byelectrical impedance spectroscopy"; **Colloids and Surfaces A: Physicochem. Eng. Aspects, (364) 132–137 (2010)**
21. Digby D. Macdonald; "Reflections on the history of electrochemical impedance spectroscopy"; **Electrochimica Acta, (51) 1376–1388 (2006)**
22. D.J. Gavaghan, A.M. Bond; "A complete numerical simulation of the techniques of alternating current linear sweep and cyclic voltammetry: analysis of a reversible process by conventional and fast Fourier transform methods"; **Journal of Electroanalytical Chemistry,(480) 133–14 (2000)**
23. National Centre For Catalysis Resaearch; Indian Institute of Technology Madras; Electrochemical Spectroscopy
24. C.D. Lokhande, T.P. Gujar, V.R. Shinde, Rajaram S. Mane, Sung-Hwan Han; "Electrochemical supercapacitor application of pervoskite thin films"; **Electrochemistry Communications, (9) 1805–1809 (2007)**
25. Sumeet Bhargava; "Temperature and gas sensing characteristics of graphite/ polymer (PEO) based composite structures"; MS thesis, University of Cincinnati
26. Yunusa A Balogun; 'Enhanced percolative properties from controlled filler dispersion an conductive polymer composites"; PhD thesis, University of Cincinnati
27. Shevchenko V.G, Ponomarenko A.T, Enikolopyan N.S; "Anisotropic effects in electrically conducting polymer composites"; **Int. J Appl. Electromagnetics in Matl.,(5) 267-277 (1994)**

28. S.K. Tripathi , Ashok Kumar , S.A. Hashmi; “Electrochemical redox supercapacitors using PVdF-HFP based gel electrolytes and polypyrrole as conducting polymer electrode”; **Solid State Ionics (177) 2979–2985 (2006)**
29. Jayesh G Bokria, Shulamith Schlick; “Spatial effect in the photodegradation of poly(acrylonitrile-butadiene-styrene): A study by ATR-FTIR”; **Polymer, (43) 3239-3246 (2002)**
30. Libuse Brozova´, Petr Holler, Jana Kova´rˇova´, Jaroslav Stejskal, Miroslava Trchova; “The stability of polyaniline in strongly alkaline or acidic aqueous media”; **Polymer Degradation and Stability, (93) 592 – 600 (2008)**
31. Yibing Xie, Degang Fu; “Supercapacitance of ruthenium oxide deposited on titania and titanium substrates”; **Materials Chemistry and Physics, (122) 23–29 (2010)**
32. Guo-Qing Zhang, Yong-Qing Zhao, Feng Tao, Hu-Lin Li; “Electrochemical characteristics and impedance spectroscopy studies of nano-cobalt silicate hydroxide for supercapacitor”; **Journal of Power Sources, 161 723–729 (2006)**
33. Yunusa A. Balogun, Relva C. Buchanan; “Enhanced percolative properties from partial solubility dispersion of filler phase in conducting polymer composites (CPCs)”; **Composites Science and Technology ,(70) 892–900 (2010)**
34. Hongyu Mi, Xiaogang Zhang, Sudong Yang, Xiangguo Ye, Jianming Luo; “Polyaniline nanofibers as the electrode material for supercapacitors”; **Materials Chemistry and Physics, (112) 127–131 (2008)**
35. Shuangli Zhou,Shanshan Mo, Wujun Zou, Fengping Jiang, Tianxiang Zhou, Dingsheng Yuan; “Preparation of polyaniline/2-dimensional hexagonal mesoporous carbon composite for supercapacitor”; **Synthetic Metals xxx, xxx– xxx (2011)**

36. Bin Dong, Ben-Lin He, Cai-Ling Xu, Hu-Lin Li; "Preparation and electrochemical characterization of polyaniline/ mulit-walled carbon nanotubes composites for supercapacitor"; **Materials Science and Engineering B, (143) 7-13 (2007)**
37. H.K Chaudhari, D.S. Kelkar; "Investigation of structure and electrical conductivity in doped aniline"; **Polymer International , (42) 380-384 (1997)**